JPL PUBLICATION 81-15

Distributed Control of Large Space Structures

David B. Schaechter

May 1, 1981

National Aeronautics and
Space Administration

Jet Propulsion Laboratory
California Institute of Technology
Pasadena, California

JPL PUBLICATION 81-15

Distributed Control of Large Space Structures

David B. Schaechter

May 1, 1981

National Aeronautics and
Space Administration

Jet Propulsion Laboratory
California Institute of Technology
Pasadena, California

The research described in this publication was carried out by the Jet Propulsion Laboratory, California Institute of Technology, under contract with the National Aeronautics and Space Administration.

Acknowledgements

The author wishes to acknowledge Dr. Connie Weeks for the contribution of the section on shape control, and Dan Eldred, for the contribution of the section on the finite element model for the flexible beam experiment. I also want to thank Dr. Massih Hamidi, Dr. Guillermo Rodriguez, and Dr. Jer Nan Juang for the many valuable discussions. In development of the flexible beam facility, Steve Gunter, George Hotz, Ed Kan, Mark Nelson, Gary Parker, Jeff Schroeder, and Dr. Eldred Tubbs were all a vital part of a team effort.

Abstract

This report represents the culmination of work to date in the areas of modeling and control of large space structures. Both theoretical developments and the results of laboratory experiments are treated herein, as they apply to active attitude and vibration control, as well as static shape control. Modern control theory has been employed throughout as the method for obtaining estimation and control laws.

Table of Contents

		Page
List of Illustrations		vii
List of Tables		viii
Nomenclature		ix
1.0	Introduction	1
1.1	General Background	1
2.0	Modeling of Large Space Structures	4
2.1	Introduction	4
2.2	Partial Differential Equation Models (PDE)	4
2.3	Finite Element Models (FE)	5
2.4	Finite Difference Models (FD)	6
2.5	Modal Models	6
3.0	Optimal Control	8
3.1	Design Procedure	8
3.2	Sensors and Actuators	8
3.3	On-Board Implementation	9
4.0	Active Control	10
4.1	Introduction	10
4.2	Necessary Conditions for Optimal Local Control	10
4.3	Finite Element Structural Models Control Design	13
4.4	Examples of Local Control Systems	15
4.5	Local Control Based on PDE Models	24
4.6	Flexible String Example	28
5.0	Shape Control	37
5.1	Introduction	37
5.2	The General Boundary Value Problem & Green's Function	38
5.3	The General Shape Control Problem	41
5.4	The General Shape Estimation Problem	43
5.5	Examples of Static Shape Estimation and Control	45
5.6	Approximations for Shape Estimation and Control	59
6.0	Experimental Verification of Distributed Control Concepts	60
6.1	Introduction	60
6.2	Dynamic Analysis of Flexible Beam Facility	62

Table of Contents (continued)

	Page
6.3 Control System Hardware and Software	75
6.4 Control Law Design	77
7.0 Future Work	82
References	83

List of Illustrations

1 Two Mass Model 16

2 Control System Design Results 17

3 Free-Free Flexible Beam 18

4 Discretized Beam Model 19

5 Full State and Local Position Feedback to Actuator 1. 20

6 Full State and Local Position Rate Feedback to Actuator 1 21

7 Full State and Local Position Feedback to Actuator 2. 22

8 Full State and Local Position Rate Feedback to Actuator 2 23

9 Operator vs. Discretized Control System Design Results (constant weight). 32

10 Operator vs. Discretized Control System Design Results (variable weight). 33

11 Operator vs. Discretized Control System Design Results (low gain) 36

12 The Simply Supported Beam 46

13 The Green's Function for the Simply Supported Beam. 48

14 Optimal vs. Desired Shape for the Simply Supported Beam 50

15 Green's Function for the Pinned-Free Beam 56

16 Shape Estimation with Rigid Body Modes. 57

17 Shape Estimation Results. 58

18 Beam Support Configurations 61

19 Beam Support Structure. 61

20 Sensor/Actuator Mounting Bracket. 63

21 Beam Mode Shapes. 66

22 Finite Element Beam Model 68

23 A Single Finite Element 68

24 Controlled and Uncontrolled Beam Responses. 80

25 Unstable Control System 80

List of Tables

I Control System Design Results 16

II Tower Resonances. 62

III Beam Characteristics. 74

IV Normal Mode Frequencies of Beam 74

Nomenclature

English

A	state weighting matrix
B	control weighting matrix
B	boundary condition operator
C	control gain matrix
D	differential operator
E	Young's modulus
f	force
f_n	nth modal force
F	concentrated force
F	dynamics matrix
g	acceleration of gravity
g	Green's function
G	control distribution matrix
H	measurement matrix
H	Hamiltonian
I	moment of inertia
I	identity matrix
j	$\sqrt{-1}$
J	scalar performance index
J	Bessel function
k	stage variable
K	estimator gains
K	stiffness matrix
ℓ,L	length
L	linear operator
m	number of controls

M	total mass
M	mass matrix
n	number of states
p	number of sensors
P	Ricatti solution
P	arbitrary point
q	modal amplitude
Q	spectral density of process noise
Q	arbitrary point
R	spectral density of measurement noise
S	sweep solution matrix
t	time variable
T	sample period
T	torque
T	linear operator
u	control
u	static deflection
u	arbitrary function
v	arbitrary function
v	measurement noise
w	process noise
x	spatial variable
x	state vector
x	state covariance matrix
y	spatially continuous state variable
y	deflection
z	measurement vector
z	normalized deflection

Greek

α	constant vector
Γ	process distribution matrix
Γ	boundary of Ω
δ	Dirac delta
λ	eigenvalue
λ	adjoint variable
Λ	Lagrange multiplier matrix
Λ	diagonal matrix of eigenvalues
μ	Lagrange multipliers for gain constraints
ξ	spatial variable
ξ	damping ratio
π	3.141592 . . .
ρ	density
ϕ	eigenvector matrix
ϕ	shape function
Φ	state transition matrix
ψ	desired shape
ω	natural frequency
Ω	spatial domain

Symbols

$(\dot{})$	time differentiation
$(\,)'$	spatial differentiation
$\frac{\partial}{\partial}$	partial derivative
δ	variation
E	expected value operator

$\sum$	summation
$(\, , \,)$	inner product
$\| \quad \|$	norm
$(\,)^{T}$	transpose
$(\,)^{-1}$	universe
$(\,)^{+}$	adjoint
$(\hat{\ })$	estimate
$(\,)_{max}$	maximum value
$(\,)_{avg}$	averaged value

Section 1

1.0 Introduction

1.1 General Background

As spacecraft became larger and more flexible, the equations needed to accurately model the static and dynamic behavior of these spacecraft became more complex. In general, higher order finite element models must be synthesized by the structural analysts in response to spacecraft tending away from lumped mass configurations and tending toward continuously distributed configurations. More and more structural modes or degrees of freedom are passed on to the control analysts in an attempt to retain a faithful model. The use of these models directly for the purpose of on-board estimation and control of attitude, shape, and station may become unwieldy. On the other hand, serious well known stability problems may arise due to the use of oversimplified models.[1]

Spacecraft size also is not the only driver of model complexity. As more demands are made of control system performance, in terms of attitude accuracy, pointing accuracy, stability, shape accuracy, slew speed, etc., structures which heretofore have been modeled as rigid bodies must now include flexibility terms. This results from the fact that as more performance is required from a given space structure, improved knowledge of the structure itself is vital, just as are more accurate sensors, actuators with better resolution, better computational accuracy and resolution, and a better understood disturbance environment.

Prior to this work, very little information was available on the control of large distributed structures. That is, assuming that any sensor/actuator arrangement and type were available, the control logic for processing the sensor outputs to produce actuator commands had not been developed. The purpose of this work was to obtain a better understanding of the theory of the control of distributed parameter systems (DPS) through analysis and laboratory experimentation. Rather than attacking the analysis problem by "building up" a general DPS from many discrete, interconnected, lumped systems, and applying existing modern control theory, new optimal control

approaches based on continuum models were developed for static and dynamic control. Using these new approaches, much insight could be gained for the control of general DPS modeled with finite elements.

There are many possible applications for spacecraft that can be modeled as DPS. Some of these include antennas, solar arrays, platforms, and solar sails. Using antennas, a broad range of the electromagnetic spectrum can be covered. Wrap-rib, hoop-column, and sunflower antenna designs may all be represented as DPS, and have applications in the microwave, radio, and x-ray bands. Solar arrays have applications ranging anywhere from power supplies for satellites to orbiting solar power stations for entire cities. Platform structures may provide common utilities including power, thermal regulation, communications, and attitude control, for a number of different experiments. Finally solar sails may some day provide an economical method of developing low thrust over long time periods.

In an effort to mimic many of the dynamic and control characteristics of DPS, a laboratory facility has been assembled. The "spacecraft" consists of a hanging flexible beam. The beam is instrumented with position sensors and force actuators. A microprocessor directs the entire control sequence for shape control and vibration control. Laboratory demonstration and verification of various control system concepts will continue to be a vital part of the large space structure control effort.

The work contained in this report on DPS can be divided into five major areas:

1) Modeling
2) Optimal Control
3) Active Control
4) Shape Control
5) Experimental Verification

The section on modeling consists of several of the more popular methods of mathematically representing physical systems for control system design purposes. The section on Optimal Control consists of a brief description

of some of the modern control approaches. Active Control refers to the control of systems governed by a set of dynamic equations of motion. This may include vibration suppression, attitude maneuvers, translation or station keeping maneuvers, etc. Shape Control means the control of an elastic structure to produce a given static shape. Finally, a section on Experimental Verification contains a description of the development and results of a facility designed to demonstrate and verify various control system design approaches.

Section 2

2.0 Modeling of Large Space Structures

2.1 Introduction

The design of a control system for any physical system must certainly begin with some knowledge of the system itself. A mathematical representation of the system, structure, or spacecraft, is known as a model. The modeling techniques to be examined in this section are partial differential equation models, finite element models, finite difference models, and modal models. Each type of model has its own merits and shortcomings depending upon the particular application. In an effort to keep all the notation simple, undamped and non-rotating structures will be considered throughout the remainder of this work. Although this type of model will not be universally applicable it will still represent a very large class of proposed large structures.

2.2 Partial Differential Equation Models (PDE)

The PDE is the most natural way of describing the behavior of a spatially continuous system, and, in fact, it will be the only continuous modeling approach to be discussed in this work. PDE's can be very useful for modeling simple systems, such as strings, beams, plates, diaphragms, shells, columns, etc., but rapidly lose their usefulness for complicated structures. The reader should be reminded that there are many complicated structures that may be represented approximately using the simple models listed above. The primary value of the PDE model for control purposes is that a PDE is a very concise approach to handling a continuous model, i.e., a model that retains an infinite number of degrees of freedom. Much insight into the control of general structures may be gained from the analysis of several "complete" models.

The general form for the PDE model considered here is given in (1).

$$\begin{aligned} \rho(x)\,\ddot{y}(x,t) &= L\,y(x,t) + f(x,t) \\ B\,y\,(\Gamma,t) &= 0 \\ y(x,t_o) &= y_o \end{aligned} \qquad (1)$$

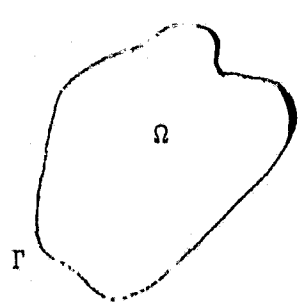

The complete model consists of equations of motion, boundary conditions, and initial conditions. In other words, (1) can be stated as "the mass times the acceleration of a point x in Ω is equal to the applied forces." These forces are due to internal forces and external forces. The dynamics are also governed by an appropriate set of boundary and initial conditions. The problem of static shape control may be incorporated into (1) by suppressing the time dependence.

2.3 Finite Element Models (FE)

The finite element modeling approach is a Lagrangian approach used to assemble the differential equations of motion for complicated structures from a set of simple elements, such as beams, plates, rods, point masses, etc.

The basis of the finite element approach is that the kinetic and potential energies in a structure can be obtained as the sum of the energies of the individual elements, and that the energies in individual elements may be approximated using a (small) finite number of discrete coordinates, and some fixed continuous interpolation functions. The energy in a particular element results from a spatial integration over the element, effectively allowing the energy to be written as a function of these variable discrete coordinates, and of some fixed constants that result from the integration process. Applying Lagrange's approach for deriving the equations of motion results in

$$M\ddot{x} + Kx = F \tag{2}$$

Attitude control, stationkeeping, and shape control of many structures can be incorporated in the format in (2).

The advantage of the finite element method of modeling is that models for arbitrary structures may be synthesized from much simpler component pieces. The mating of various components, as well as the boundary conditions of the overall structure are satisfied "automatically." Furthermore, a great deal of software has been developed for assembling high order models,

and for performing the subsequent analysis. One disadvantage of finite element modeling is that the model itself may be very high order, (perhaps hundreds), and that useable results can only be obtained after an eigensystem analysis of the high order model.

2.4 Finite Difference Models (FD)

A finite difference model is a direct approach to deriving equations of motion, as opposed to the variational approach analyzed with FE. The finite difference method is the result of approximating a differential operator directly by means of finite differences. In general, therefore, the higher the order of the operator, the more coupled the dynamics of a given point is with adjacent points. General boundary conditions can only be enforced by painstakingly obtaining the FD equation that is also consistent with the desired boundary value. It is not possible using FD techniques to assemble complex models using simple components, as is the case with FE. FD modeling for large structures has only very limited usefulness. The general form for a finite difference model is the same form as (2), except that the mass matrix with FD is diagonal.

2.5 Modal Models

A modal model of a structure is usually the output of another modeling process, generally PDE, FE, or FD. Modal models yield a decoupled set of second order differential equations describing the natural or unforced behavior of the structure, in terms of the modal amplitudes. Because of the fact that the natural modes of a system are easily observed, much insight can be gained by study of a modal model. Under the assumption that any motion of the system can be represented as some time varying linear combination of the modes, knowledge of the mode shapes and their time varying amplitude is sufficient to completely describe arbitrary behavior. The inhomogeneous modal model of the time varying amplitudes is usually written

$$\ddot{q}_n + \Omega_n^2 \, q_n = \int \phi_n(x) f(x,t) \, dx \qquad (3)$$

where the eigensystem analysis is either performed analytically in the case of PDE, or numerically (using a wide variety of available software) in the case of FE or FD models.

For the aforementioned reasons, it would appear that modal models are ideal for controls applications, being natural and simple in structure. In fact, modal models had enjoyed widespread usage up to and including their application to large structure control. The particular problem encountered with the use of modal models is that in theory, an infinite number of modes are required to model a continuous structure, whereas in practice, it is only possible to work with some finite number. Truncation of the series approximation of the model may result in system instability, inasmuch as these modes are still forced by outside forces, but the resulting motion was previously assumed to be unimportant.

Section 3

3.0 Optimal Control

3.1 Design Procedure

The primary reason for adding a control system to a system or a structure is to change the characteristics of that system, whether it be in response to commands, or in response to disturbances. Evidently, there are changes in the system that can be made which makes its characteristics closer to some desired performance, and there are other changes that make the performance less desirable. One method of specifying a measure of performance in the control system design process is through control system design methods using optimal control.

The optimal control design process involves specification of a scalar performance measure or cost function that reflects the relative importance of a variety of different factors. The choice of feedback control law that minimizes the cost function is then deemed to be "the optimal control."

The form of the cost function used throughout this work is a quadratic performance index. That is to say, a quadratically increasing cost is incurred for both (1) using additional control effort, and (2) desired outputs from the system not matching actual outputs.

Quadratic cost functions yield easily implemented linear state estimators and controllers. Furthermore, an entire body of information exists for the theory, performance, and implementation of this type of controller.

3.2 Sensors and Actuators

The purpose of this work is to address the theory of the control of large structures. The two major reasons for the need of a new theory of control is that future large space structures differ from present day structures in two very significant aspects. First, the control of large structures involves the control of systems governed by continuum or infinite dimensional models, and second, even a simplified model of the structures is likely to contain gross errors due to the inability of conducting meaningful ground tests of these large structures.

The problem of designing new sensors and actuators, or, of selecting them from existing sensor/actuator technology is not addressed in this work. When needed, it will be assumed that ideal position sensors, angle sensors, rate sensors, torquers, etc. will be available for the control system design process.

3.3 On-Board Implementation

As with the sensors and actuators, very little attention will be paid to the on-board implementation of the control system. It is implicitly assumed, however, that an on-board ditigal computer will be available for implementing the control law, if necessary. In a qualitative sense, it will be recognized that there are limitations to the computational capability of the on-board processor, whether the processor is physically in the form of a single, lumped computer, or if it consists of a distributed matrix of smaller processors.

Section 4

4.0 Active Control

4.1 Introduction

This section contains a derivation of the necessary conditions for an optimal local control law for a general system in state variable format. A local control law is one in which only local state information is used to synthesize the control law for each actuator (even if additional state information is available) and hence, is a different problem from that of output feedback.[2,3] A practical application of this idea occurs in designing control systems for large flexible space structures, where many sensor outputs may be available for feedback, yet it is not practical to do so due to the large spatial distances involved.

By representing the structure in physical coordinates (the initial output of the PDE,FD or FE analysis) rather than modal coordinates, the numerical solution of the optimal full state and local feedback problems may be simplified. Numerical examples of control law designs for a simple two mass model, for a free-free flexible beam, and for a string in tension are given. Similar examples using different design approaches may be found in References 4 and 5.

The counterpart to the local control law is a local estimation scheme. Local estimation processes sensor information using a dynamic model of the system to obtain estimates of only the nearby components of the state vector, not the entire state vector. These components of the estimated state vector should be precisely those components required by the local control law. Combining the local state estimator with the local control law results in a local controller which significantly reduces the amount of on-board computation, and allows the computations to be performed in a distributed or parallel manner.

4.2 Necessary Conditions for Optimal Local Control

The derivation of the necessary conditions for the optimal local control begins with a system in state variable format and a quadratic performance index to be minimized as is shown in (4).

$$\dot{x} = Fx + Gu + w \qquad x(t_o) \text{ given}$$
$$\min_u J = 1/2 \int_{t_o}^{t_f} (x^T Ax + u^T Bu)\, dt \tag{4}$$

Assuming that the desired final solution is of the form $u = Cx$, the substitution into (4) is made yielding the deterministic equivalent

$$\dot{x} = (F + GC)\, x \qquad x(t_o) \text{ given}$$
$$\min_C J = 1/2 \int_{t_o}^{t_f} x^T (A + C^T BC)\, x\, dt \tag{5}$$

At this point, the constraint that only local states be fed back can be enforced by requiring that certain components of C be identically zero and that the minimization in (5) be carried out with respect to the remaining, non-zero components of C. Equivalently, the constraints may be adjoined to the Hamiltonian to yield

$$H = 1/2\, x^T (A + C^T BC)\, x + \lambda^T (F + GC)\, x + \mu_{ij} C_{ij} \tag{6}$$

where

$$\mu_{ij} = 0 \quad \text{if} \quad C_{ij} \neq 0$$

$$\mu_{ij} \neq 0 \quad \text{if} \quad C_{ij} = 0$$

and where summation over the repeated indices is implied. The optimality condition becomes

$$BC\, xx^T + G^T \lambda\, x^T + \mu = 0 \tag{7}$$

where the μ_{ij}'s are picked to make the corresponding constrained C_{ij}'s equal to zero.

The usual sweep solution obtained by letting

$$\lambda(t) = S(t)\, x(t), \quad C = - B^{-1} G^T S(t) \tag{8}$$

no longer works in general since the optimality condition in (7) results in C being a function of x and t, i.e. the minimization can no longer be performed independently of the initial condition. However, the appearance

of the terms xx^T and λx^T above suggests that a linear statistically optimal control may exist. The stochastic analog of (5) in terms of the covariance of the state is[6]

$$\begin{aligned} &\dot{X} = (F + GC)\, X + X\, (F + GC)^T + Q \qquad X(t_o) \quad \text{given} \\ &\underset{C}{\text{Min}}\ J = \text{trace} \int_{t_o}^{t_f} 1/2\ (AX + C^T\, BC\, X)\, dt \end{aligned} \tag{9}$$

where designated C_{ij}'s are zero and $X = E(xx^T)$. The accomplishment in the preceding step is to average the performance index over a range of possible initial conditions. Rather than considering all initial conditions to be equally likely,[7] a more realistic range of possible initial states can be obtained using the state covariance matrix. The adjoint matrix equation and optimality condition are:

$$\begin{aligned} &-\dot{\Lambda} = \Lambda\, (F + GC) + (F + GC)^T\, \Lambda + A + C^T\, BC \qquad \Lambda(t_f) = 0 \\ &BC\, X + G^T\, \Lambda\, X + \mu = 0\ . \end{aligned} \tag{10}$$

Although an exact solution to (10) is possible, an approximate solution may be easily obtained by expanding the equations in (10) to first order in μ about the optimal solution for $\mu = 0$. This yields

$$C(t) \cong - B^{-1} [G^T\, \Lambda(t) + \mu\, X^{-1}(t)] \tag{11}$$

where Λ and X are the solutions of the unconstrained optimal control problem ($\mu = 0$), and μ is picked to zero the corresponding components of C. For the unconstrained problem, $\mu = 0$, the result in (11) reduces to the familiar result, $C=-BG^T\Lambda$. Equation (11) has a nice physical interpretation. To first order in μ, if not all the states can be fed back, those states that are available should be fed back with a correction to the feedback gains based on the correlation between those states fed back, and the remaining states. (As a practical note, the inverse in (11) need never be computed. In fact only "a few" elements of X need to be manipulated.) Furthermore, since the solution is expanded about the optimal solution, it can be shown that $\frac{\partial J}{\partial \mu_{ij}} = 0$, i.e. this concept of local control does not severely affect performance to first order in μ. The algorithm for solving the local

control problem can be outlined as follows. First, solve the full state optimal control problem, next, apply the local control correction appearing in (11).

It should be noted that as in the full state feedback case, for F, G, A, B, and Q all constant, it is possible that a steady state solution for C, A, and X may be obtained as $t_f - t_o \to \infty$. However, as opposed to the case of full state feedback, stability of the closed loop system is not guaranteed when using local control gains. The eigenvalues of F + GC using the local control gain must be determined to verify stability of the closed loop system.

Thus far, the problem of solving the full state optimal control problem (step one above) for high order systems has been avoided. However, the solution procedure required usually assumes that a low order model of the high order system is available to make the problem tractable. Traditionally, the structural analyst supplies as many modes as the control system designer wishes. Regardless of where the actual truncation occurs, or by what method, the control system designer begins with a deficient model. This may result in closed loop instabilities.

The alternative to working with the truncated system model is working with a full order finite element model, as it is generated by the structural analyst. The next section offers some hope that the analysis of these high order systems, particularly structural systems, may be feasible.

4.3 Finite Element Structural Models Control Design

In an attempt to develop control system design techniques for high order systems, and to alleviate the problem of truncated modes, it is worthwhile to examine the structural equations of motion. Attitude control, station-keeping, and figure control of many structures can be represented by the following matrix equation.

$$M\ddot{x} + Kx = Gu \tag{12}$$

Matrix bandedness of M and K is a direct result of the finite element modeling. Since control inputs from a given actuator are applied at a single station on the structure, nearly all of the elements of G are zero.

Equation (12) can be placed in modal form

$$\ddot{q} + \Omega^2 q = \phi^T G u \tag{13}$$

by normalizing the eigenvector matrix, ϕ, so that

$$\begin{aligned} x &= \phi q \\ \phi^T M \phi &= I \\ \phi^T K \phi &= \Omega^2 \end{aligned} \tag{14}$$

where Ω is a diagonal matrix of modal frequencies. Furthermore, computer programs like EIGSOL[8] and DAMP[9] can solve the open loop eigenvalue problem ($u = 0$ in (12)) very efficiently by taking full advantage of the matrix sparsity in both storage and computation.

Consider now the problem of designing a control system for the system in (13). Selection of a control law can be based on the minimization of a quadratic performance index similar to that appearing in (4).

$$J = 1/2 \int_{t_o}^{t_f} (x^T A x + u^T B u)\, dt \tag{15}$$

Regardless of where or if truncation of the modal system occurs, the open loop system dynamics matrix, Ω^2, is a diagonal matrix and hence, simple to manipulate from a computational point of view. However, the corresponding control distribution matrix $\phi^T G$ is not a sparse matrix, and so the Hamiltonian system for the corresponding optimal control problems has the following form

$$\begin{bmatrix} \Omega^2 & \phi^T G B^{-1} G^T \phi \\ A & \Omega^2 \end{bmatrix} \tag{16}$$

The shaded areas in (16) represent non-zero matrix entries. Because little useful matrix structure remains in (16), the eigensystem analysis required for the solution of the optimal control problem can not be performed efficiently. Consider instead the control of the original dynamic system in (12). At this point the concept of local control emerges naturally. The dynamics of the flexible structure are characterized locally. This is

the reason that a good dynamic model of the flexible structure can be obtained using tightly banded matrices. Furthermore, actuators produce effects locally, and sensors measure local behavior. It therefore seems plausible that a good controller may be possible using only local state information.

The optimal control problem may be formulated as follows.

$$\begin{aligned} &\ddot{Mx} + Kx = Gu && x(t_o),\ \dot{x}(t_o) \quad \text{given} \\ &\min_u J = 1/2 \int_{t_o}^{t_f} (x^T Ax + u^T Bu)\, dt \end{aligned} \tag{17}$$

By adjoining the constraints in (17) to the performance index with Lagrange multipliers, λ, and integrating by parts, two times, the closed loop system dynamics and the corresponding matrix structure are given by

$$\begin{bmatrix} M & 0 \\ 0 & M \end{bmatrix} \begin{bmatrix} \ddot{x} \\ \ddot{\lambda} \end{bmatrix} + \begin{bmatrix} K & -GB^{-1}G^T \\ A & K \end{bmatrix} \begin{bmatrix} x \\ \lambda \end{bmatrix} = \begin{bmatrix} 0 \\ 0 \end{bmatrix} \qquad \begin{matrix} x(t_o),\ \dot{x}(t_o) \text{ given} \\ \lambda(t_f) = \dot{\lambda}(t_f) = 0 \end{matrix} \tag{18}$$

$$\begin{bmatrix} \ddots & \\ & \ddots \end{bmatrix} \begin{bmatrix} \ddot{x} \\ \ddot{\lambda} \end{bmatrix} + \begin{bmatrix} \ddots & \\ & \ddots \end{bmatrix} \begin{bmatrix} x \\ \lambda \end{bmatrix} = \begin{bmatrix} 0 \\ 0 \end{bmatrix}$$

Equation (18) is the Hamiltonian system corresponding to the optimal control problem in (17). The important feature to notice is that nearly all of the original system's matrix structure is preserved, and that the eigensystem analysis that must be performed in (18) to obtain the optimal control differs from that which must be performed in (17) to analyze the open loop system dynamics, by only two "stripes" off the principal diagonal. As such, from a computational point of view, both storage and computation time can be reduced by fully exploiting the high degree of matrix sparsity in an eigensystem analysis or through efficient matrix perturbation techniques.

4.4 Examples of Local Control Systems

This section contains two examples of the steady state optimal local control concept and comparisons of the performance of the optimal local

control law with the performance of control laws designed using various other approaches.

Example I - Two Mass Model

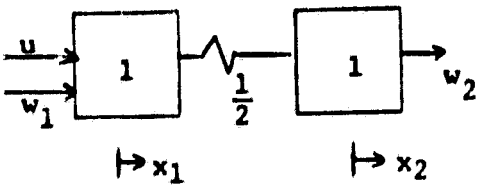

$$\min E(J) \qquad J = 1/2 \int_0^\infty x_1^2 + 4u^2 \, dt \qquad Q = I_2$$

Fig. 1 Two Mass Model System

Figure 1 consists of two unit masses connected by a spring with stiffness, one half. The open loop system has a single rigid body translation mode and a single vibration mode. It is desired to control the position of mass 1 (x_1) with a control input u, in the presence of the disturbances w.

Three approaches for designing control systems are examined:

a) Full state optimal control. All four states are available for feedback (x_1, $\dot{x}_1$, x_2, $\dot{x}_2$).

b) Modal control. The control system is designed on the basis of a rigid body model.

c) Local control. The feedback gains on x_2 and $\dot{x}_2$ are constrained to be zero.

For the given performance index, the results are most easily summarized in figure 2 and Table 1.

Table 1. Control System Design Results

	eigenvalues		gains				
Controller	Mode 1	Mode 2	X_1	$\dot{X}_1$	X_2	$\dot{X}_2$	Performance Index J
Open Loop	0,0	$\pm$ 1j	0	0	0	0	∞
Full State	-.310 $\pm$ .404j	-.128 $\pm$ .974j	-.384	-.876	-.116	-.453	3.792
Rigid Body	-.357 $\pm$ .619j	-.355 $\pm$ .606j	-.500	-1.414	0	0	4.949
Local	-.144 $\pm$ .299j	-.186 $\pm$ .984j	-.221	-.661	0	0	4.393

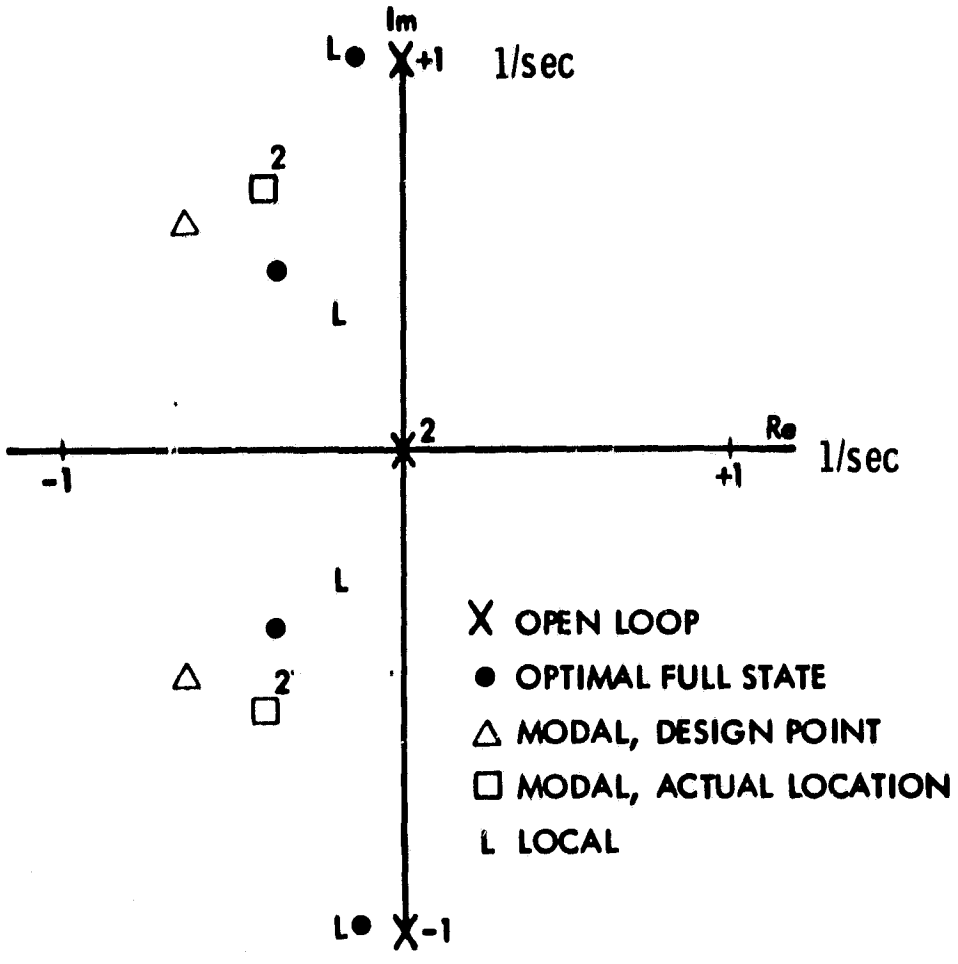

Figure 2. Control System Design Results.

The closed loop eigenvalues, feedback gains, and performance index are given for each control system design approach. Of course, the full state optimal control law "performs" the best. The desired root locations for the control system designed using the truncated dynamic model are shown in Figure 2 with triangles. Due to the presence of the truncated system dynamics (in this case the vibration mode), the four closed loop roots actually end up some distance away from the rigid body design point. The local control system is designed using the full systems dynamics, but with the constraint of partial state feedback. This closed loop system is "closer" to the optimal full state control law than is the rigid body control law in terms of both the system performance and the final root locations, and only uses feedback of x_1 and $\dot{x}_1$. It should be noted that as the cost of control decreases (B decreases), the relative merits of the local control law over the rigid body control law become even more apparent.

Example II - Free-Free Flexible Beam

The partial differential equation of motion for a free-free flexible beam with constant properties per unit length is given below (fig. 3).

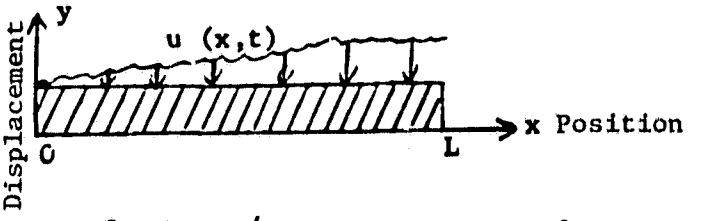

$$\rho \frac{\partial^2 y}{\partial t^2} + EI \frac{\partial^4 y}{\partial x^4} = u(x,t) \qquad \frac{\partial^2 y}{\partial x^2}(0) = \frac{\partial^2 y}{\partial x^2}(L) = 0$$

$$\frac{\partial^3 y}{\partial x^3}(0) = \frac{\partial^3 y}{\partial x^3}(L) = 0$$

Fig. 3. Free-Free Flexible Beam.

A finite difference discretization of this beam can be obtained by choosing a state vector composed of deflections and deflection rates at ten stations along the beam (fig. 4).

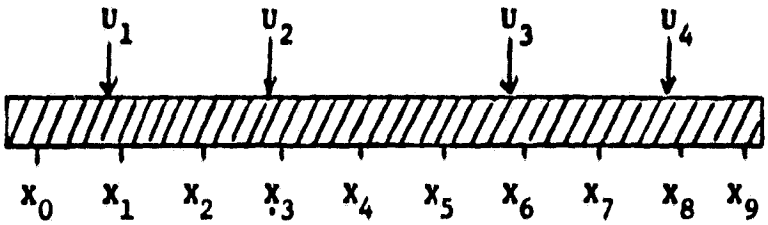

Fig. 4. Discretized Beam Model

Furthermore, it is assumed that control forces u_i can be applied at the designated stations. Penalizing the beam displacements at each of the ten stations results in a control law which performs stationkeeping, attitude control, and shape control. The following matrices were chosen for the quadratic performance index

$$A = I_{10} \qquad B = 0.01 \cdot I_4$$

As before

$$Q = I_{10}.$$

A full state optimal control law and a local control law were designed for the flexible beam using $\rho = EI = 1$, $L = 9$. Due to the symmetrical placement of the actuators, it is sufficient to present the feedback gains for synthesizing u_1 and u_2. In each of the accompanying figures (figures 5,6,7, and 8) solid lines are the full state feedback gains as a function of station location and the broken lines are the local feedback gains obtained under the constraint that only states which are immediately adjacent to the actuator are allowed to be fed back.

There are several important features of these results to recognize.

1) The full state feedback control law makes very little use of "distant" state information. This feature is not apparent from the modal approach where the feedback gains corresponding to the various modes may be roughly the same magnitude. Evidently the modal feedback effects tend to accumulate at the actuators and cancel far from the actuator.

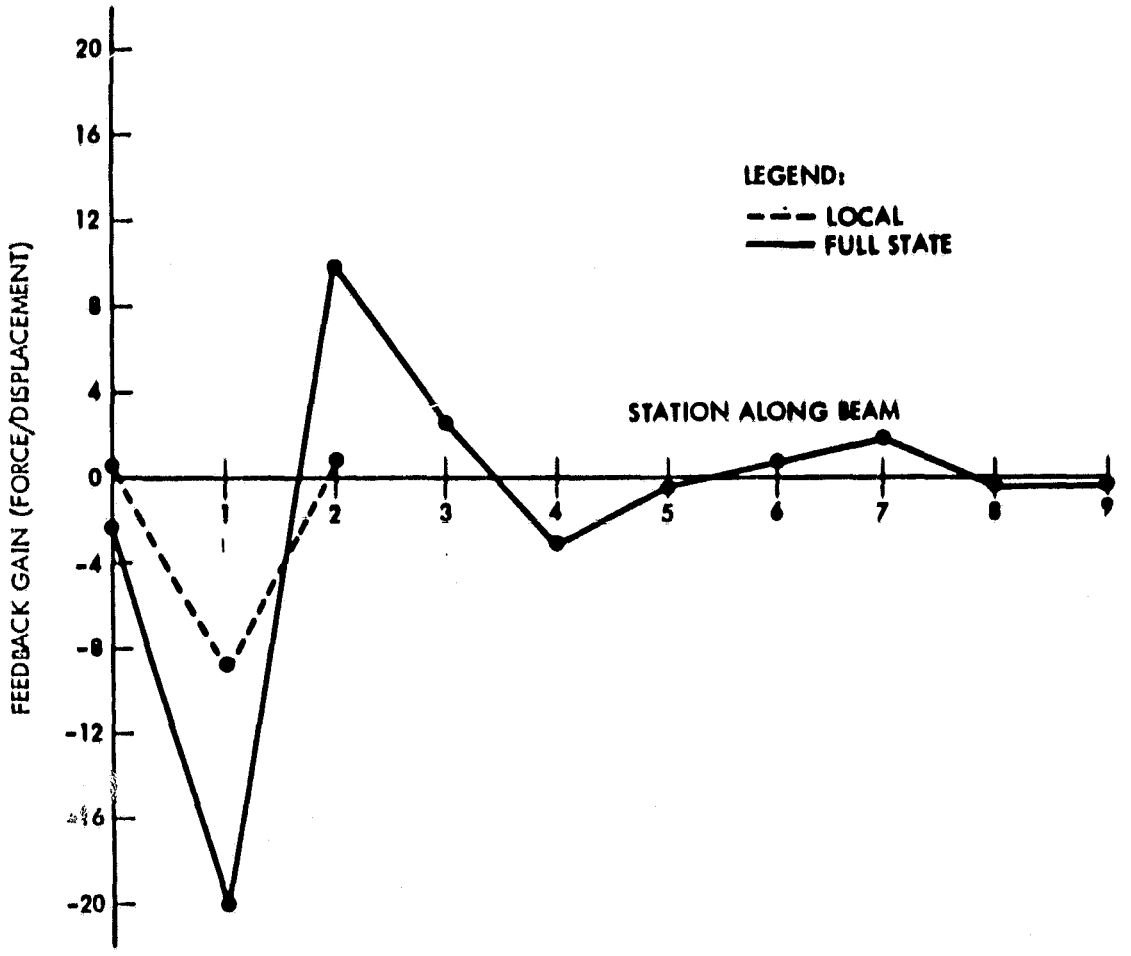

Figure 5. Full State and Local Position Feedback to Actuator 1

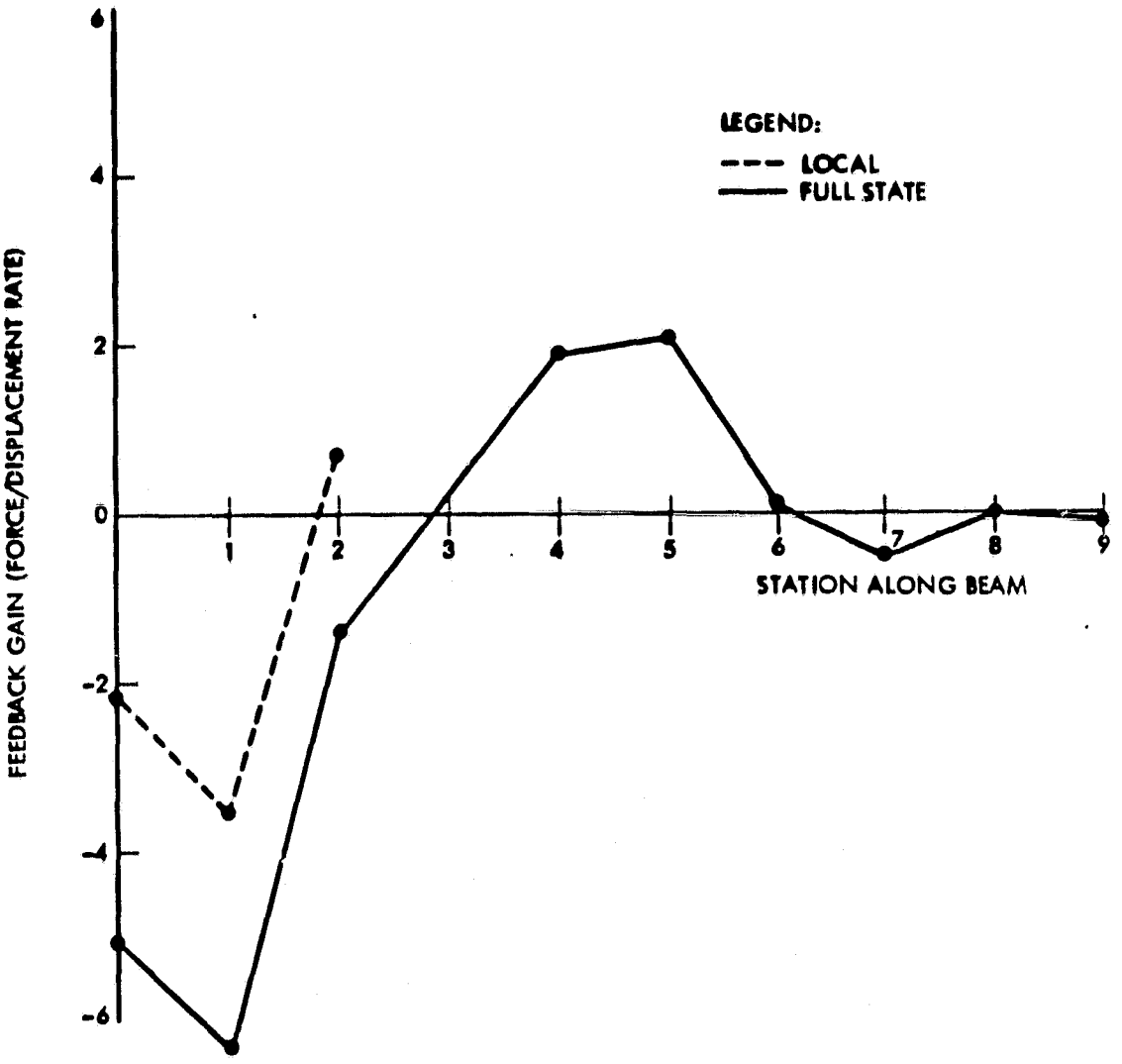

Figure 6. Full State and Local Position Rate Feedback to Actuator 1.

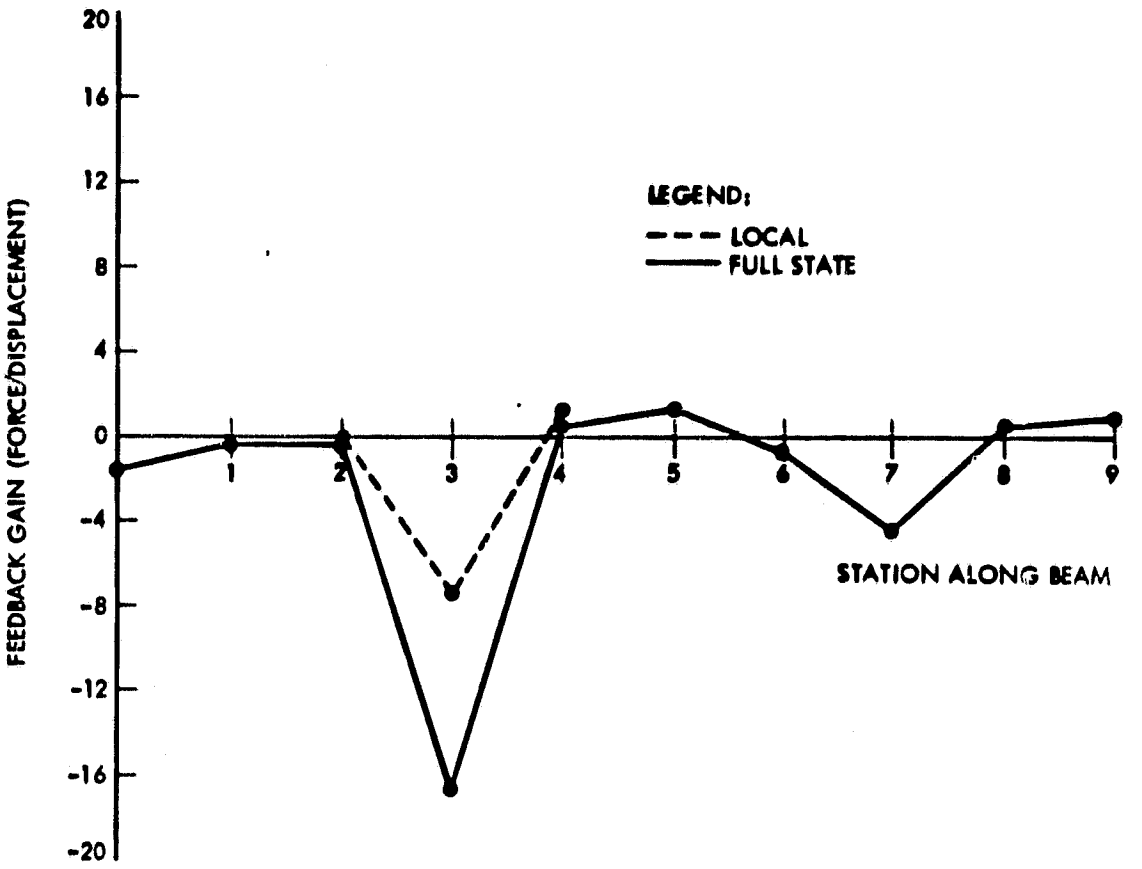

Figure 7. Full State and Local Position Feedback to Actuator 2

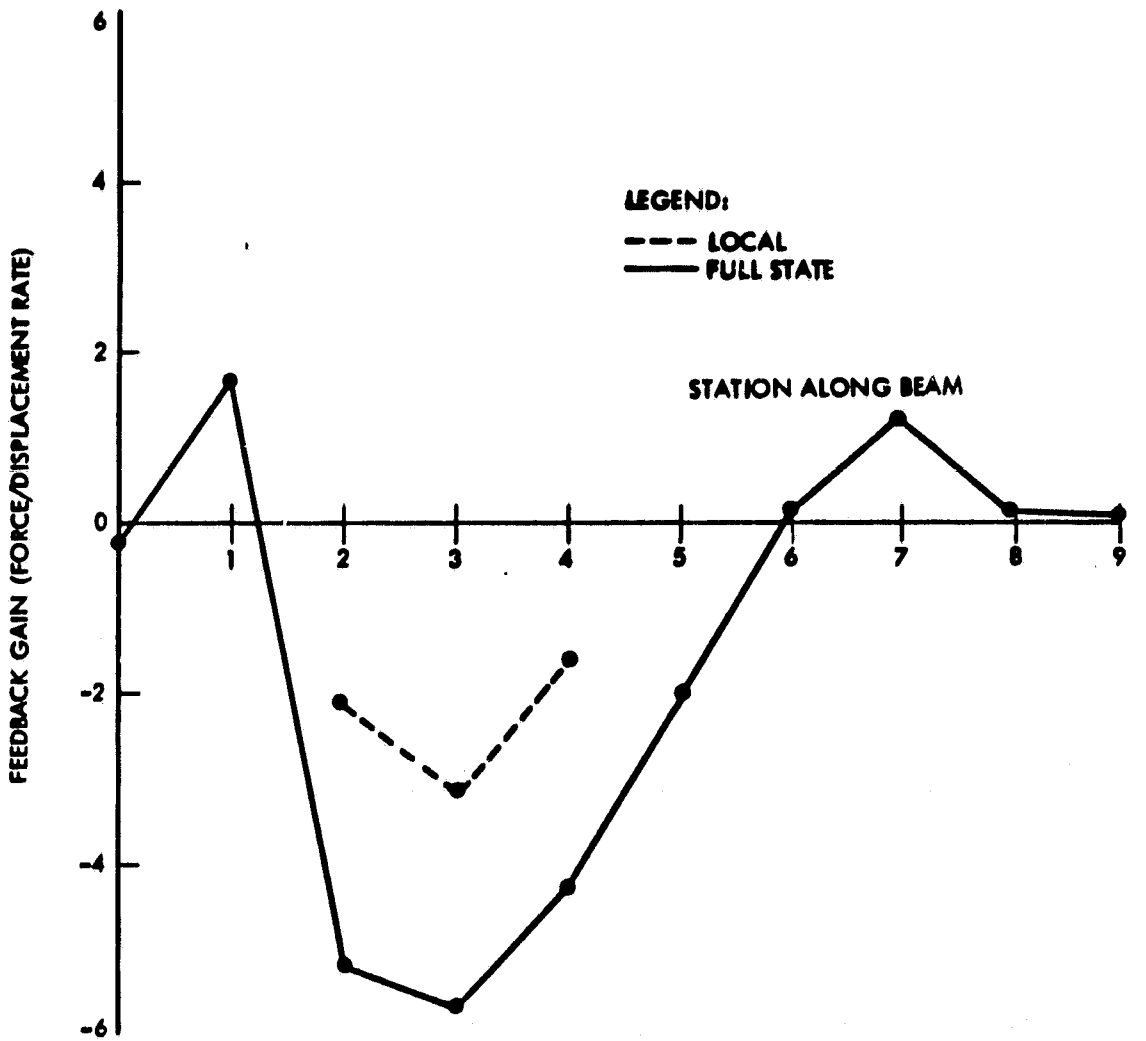

Figure 8. Full State and Local Position Rate Feedback to Actuator 2

2) The local control law is equivalent to active springs and dashpots, to provide stationkeeping, attitude control, and figure control. This result may be useful for control system design for general flexible structures.

3) In this example, the difference between the performance index using the local control in place of the full state optimal control is less than 1%. In general, the use of local control guarantees no first order change in the performance index.

4) From a computational point of view, the following computer CPU times were required by a UNIVAC 1108 to obtain the control laws for this 20-state system.

a) OPTSYS,[10] 18 seconds. The QR algorithm is applied to the 40th order Hamiltonian system to extract closed loop eigenvalues and eigenvectors.

b) Direct Integration, 15 seconds. Direct integration of the matrix Ricatti equation exploiting all matrix sparsity was employed to obtain steady state gains.

4.5 Local Control Based on PDE Models

One possible method of circumventing the problems resulting from the increased number of modes to be controlled is by avoiding modal models completely. Working directly with partial differential equation (PDE) models of continuous spacecraft is a viable alternative. In fact, some structures, such as solar panels, large antennas, and astromasts may be more easily modeled with PDE than with FE, particularly when many modes are required.

The motivation behind the "local" approach to be discussed here is that the PDE for a continuous spacecraft describes the acceleration of each physical point on the spacecraft in terms of differential operators, i.e. in terms of the behavior of the spacecraft within a local neighborhood of each point. Since sensors measure and disturbances affect local variables,

a reasonable job of state estimation may be accomplished with local state estimation. The entire design procedure would avoid entirely the problems associated with high order (possibly truncated) modal models. If it is, in fact, true that a local control law minimizes a quadratic performance index for distributed parameter system, then the underlying explanation for this certainly must be derivable from the PDE control formulation.

The control analog of this problem has already been addressed in the previous section. It has been shown that the optimal control law for a free-free flexible beam very closely resembles a local controller. This means that if a modal controller for this system is designed, the feedback law may actually represent a more simply expressed control law were it expressed in physical coordinates.

Breakwell[11] has also obtained some results for the optimal control of a continuous flexible beam using PDE, in which a symmetric root locus approach is used to determine the optimal closed loop root positions. Following this step, the continuous control gains needed to move the roots to their optimal closed loop locations remain undetermined. That is, no direct procedure is available for directly determining the optimal feedback gains.

The purpose of this section is to present a PDE estimation and control problem formulation that contains sufficient generality to encompass a wide variety of continuous control system design problems within a single analytical framework. By drawing on a simplified example, a string in tension, some insight to the control of continuous structures is obtained, and some generalizations for their control can be made. Although the estimation problem is discussed here, the results can be extended easily to include the control problem too. A procedure for the direct determination of the continuous optimal feedback gain is given, following the format used in the control of systems governed by ordinary differential equations.

Consider a general partial differential equation of motion in state variable format. This equation represents the dynamics of the state vector in some spatial domain, with boundary conditions prescribed on the boundary of this domain. The initial state of the system is given. It is desired

to obtain an estimate of the state of the system as time evolves, from noisy measurements in the presence of disturbances. The mathematical model is given below.

$$\dot{y}(x,t) = F(D)\, y(x,t) + \Gamma(x,t)w(x,t)$$

$$y(x,t_o) \quad \text{given}$$

$$B(D)\, y(\Gamma,t) \qquad \text{given}$$

$$z(x,t) = H(D)\, y(x,t) + v(x,t) \tag{19}$$

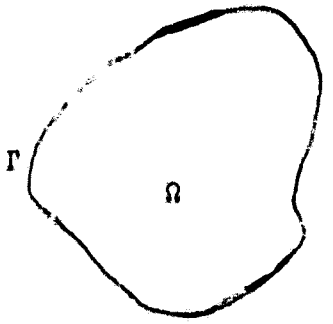

F(D), H(D), and B(D) are linear differential operators in the spatial variable. Were it not for the presence of the differential operators in (19), the mathematical formulation would be identical to the ordinary differential equation state variable format. (It will therefore be notationally convenient to omit future appearances of all superfluous symbols. It should be remembered that the model actually analyzed is written in all of its detail only in (19)). In order to obtain a state estimate from the measurements, a performance criterion is selected which weights the relative importance of the process and measurement disturbances. Minimization of this performance index is one way of obtaining the optimal state estimate.

$$J = 1/2 \int_{t_o}^{t_f} \int_{\Omega} (x^T Q^{-1} w + v^T R^{-1} v)\, dx\, dt \tag{20}$$

Adjoining the constraint dynamics in (19) to the performance index in (20) gives

$$J = \int_{t_o}^{t_f} \int_{\Omega} \{\frac{w^T Q^{-1} w + (z-Hy)^T R^{-1} (z-Hy)}{2} + \lambda^T (-\dot{y} + Fy + \Gamma w)\}\, dx\, dt \tag{21}$$

The necessary condition for the minimization of the performance index is that the first variation of J vanishes for arbitrary admissible variations. This variation yields:

$$0 = \delta J = \int_{t_o}^{t_f} \int_{\Omega} (w^T Q^{-1} + \lambda^T \Gamma)\ \delta w\ dx\ dt$$

$$+ \int_{t_o}^{t_f} \int_{\Omega} \{-\delta y^T H^T R^{-1}(z-Hy) - \lambda^T \delta \dot{y} \qquad (22)$$

$$+ \lambda^T F\ \delta y\}\ dx\ dt$$

Since δw in (22) is arbitrary, the optimality condition is obtained.

$$w = -Q\ \Gamma^T \lambda \qquad (23)$$

Two steps are now required to isolate the δy multiplier in (22). The first is to integrate the $\lambda^T\ \delta \dot{y}$ term by parts to obtain the final conditions on the adjoint variable, $\lambda^T(x,t_f) = 0$, and also an integrated term, $-\dot{\lambda}^T\ \delta y$. The second step requires the isolation of the δy terms from their operators F and H^T. A short digression is required.

Let $(\cdot,\cdot)$ define an inner product.

If T is some operator then its adjoint operator T* is defined as

$$(u,Tv) = (T^* u, v)$$

Using the star notation to denote adjoint operators, the equations for the adjoint variable becomes

$$\dot{\lambda} + F^*\lambda - H^* {}^T R^{-1}(z-Hy) = 0 \qquad (24)$$

Boundary conditions on λ will result from computation of the adjoint operator.

The closed loop dynamics of the estimator is now written below.

$$\begin{bmatrix} \dot{y} \\ \dot{\lambda} \end{bmatrix} = \begin{bmatrix} F & -\Gamma Q \Gamma^T \\ -H^T * R^{-1} H & -F^* \end{bmatrix} \begin{bmatrix} y \\ \lambda \end{bmatrix} + \begin{bmatrix} 0 \\ H^T * R^{-1} H \end{bmatrix} z$$

$$y(t_o) \quad \text{given} \qquad By = 0 \qquad (25)$$

$$\lambda(t_f) = 0 \qquad B^*\lambda = 0$$

As usual, it is desirable to write the estimator in the form

$$\dot{\hat{y}} = Fy + K\,(z - Hy) \tag{26}$$

Here K may be a differential operator estimator gain. Toward this end, let

$$y = \hat{y} - P\lambda$$

where P is also an operator. It is now straightforward to show

$$\dot{\hat{y}} = F\hat{y} + K\,(z - H\hat{y}) \qquad \hat{y}(t_o) = y(t_o)$$

$$\dot{P} = PF^* + FP + PQP^T - PH^*{}^T R^{-1} HP \qquad P(0) = 0 \tag{27}$$

$$K = PH^T * R^{-1}$$

where products of operators of course represent composite operations.

The problem of determining the optimal estimator gains for a spatially continuous system has now been reduced to a familiar format. The only differences are that the estimator gains are now in operator form, and that the Riccati equation for the estimator gain is in terms of a differential operator, P. That such a solution exists and is unique is not pursued here.[12] Rather, a detailed example problem is presented in the following section.

4.6 Flexible String Example

Consider the dynamics of the string in tension shown below.

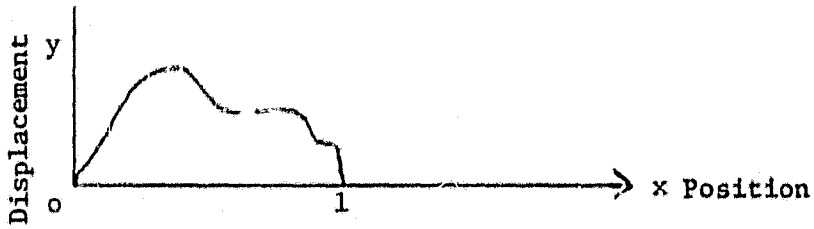

The partial differential equation of motion is given by

$$\frac{\partial^2 y}{\partial t^2} = \frac{\partial^2 y}{\partial x^2} + w \qquad y(0,t) = y(1,t) = 0 \qquad y(x,0) = 0 \tag{28}$$

Assume a continuous position measurement, z, is available, and that it is desired to find the steady state estimator that will minimize the following performance index.

$$J = 1/2 \int_0^\infty \int_\Omega (w^T Q^{-1} w + v^T R^{-1} v) \quad dx\, dt \ . \tag{29}$$

From (28) and (29), the equivalent state variable formulation is obtained as

$$F = \begin{bmatrix} 0 & 1 \\ D^2 & 0 \end{bmatrix} \quad \Gamma = \begin{bmatrix} 0 \\ 1 \end{bmatrix} \quad H = [1,\ 0] \ . \tag{30}$$

Letting

$$(u,v) = \int_0^\infty \int_0^1 uv\, dx\, dt$$

the adjoint operator to F is given by [13]

$$F^* = \begin{bmatrix} 0 & D^2 \\ 1 & 0 \end{bmatrix} \tag{31}$$

Using the results in (27) and letting

$$P = \begin{bmatrix} P_1 & P_2 \\ P_3 & P_4 \end{bmatrix}$$

it can be shown that the steady state optimal estimator can be obtained from solution of

$$\begin{aligned} &P_3 + P_2 - P_1 R^{-1} P_1 = 0 \\ &P_4 + P_1 D^2 - P_1 R^{-1} P_2 = 0 \\ &D^2 P_1 + P_4 - P_3 R^{-1} P_1 = 0 \\ &D^2 P_2 + P_3 D^2 + Q - P_3 R^{-1} P_2 = 0 \end{aligned} \tag{32}$$

Again, it is pointed out that products above denote composite operations. Even so, the feedback gains can be written symbolically as

$$K = \begin{bmatrix} P_1/R \\ P_3/R \end{bmatrix} \quad \begin{bmatrix} \sqrt{2(D^2 + \sqrt{D^4 + Q/R}} \\ D^2 + \sqrt{D^4 + Q/R} \end{bmatrix} \tag{33}$$

where the square root of an operator is to be interpreted as the operator whose composite operation with itself yields the desired operator. In each case, results obtained using the above analysis will be compared with numerical results using a discretized 20 state representation of the string dynamics, with the program OPTSYS.[10]

In the following examples, the estimator gains determined using the differential operator approach will depend on the relative norms of D^4 and Q/R in (33). Obviously the norm of D^4 defined as

$$||D^4|| = (y,D^4y)/(y,y) = (D^2y,D^2y)/(y,y)$$

can be made arbitrarily large. At this time some notion of the modal concept does prove to be useful (although it is still not required). In general, higher frequency modes in the time domain result in higher frequency mode shapes in the spatial domain. The norm of D^4 on these eigenfunctions will then serve as a basis for which modes are low frequency, and which are high frequency. What will eventually be seen is that there will be distinct estimation approaches for the high frequency modes versus the low frequency modes.

Case I $\quad Q = 10^4,\ R = 1$

For Q/R large, or alternatively, for estimation of the component motion due to low frequency behavior, an expansion of (33) gives

$$P_3/R = \sqrt{\frac{Q}{R}}\left[1 + \frac{D^2}{\sqrt{\frac{Q}{R}}} + \frac{D^4}{2\frac{Q}{R}} \cdots\right]$$

$$P_1/R = \sqrt{2}\sqrt[4]{\frac{Q}{R}}\left[1 + \frac{D^2}{2\sqrt{\frac{Q}{R}}} \cdots\right] \qquad (34)$$

Regardless of the dynamic system involved, for Q/R large, the estimator gains as a function of position are approximately constants. Since they are not "operators", they will involve feedback of only local state information. In fact, Q/R large is precisely the condition needed to guarantee the optimality of local estimation (or local control in the control problem). The estimator for this problem will then be

$$\frac{d}{dt}\begin{bmatrix}\hat{y}\\ \dot{\hat{y}}\end{bmatrix} = \begin{bmatrix}0 & 1\\ D^2 & 0\end{bmatrix}\begin{bmatrix}\hat{y}\\ \dot{\hat{y}}\end{bmatrix} + \begin{bmatrix}\sqrt{2}\sqrt[4]{Q/R}\\ \sqrt{Q/R}\end{bmatrix}(z-\hat{y}) \qquad (35)$$

Notice that the estimate error tends to zero for all modes, not just for the low frequency modes. That is to say, truncation of the differential operator to include only the leading term does not result in any instabilities. A comparison of the estimator gains obtained using the operator approach versus the discrete approximation is shown below (fig. 9).

The real power of the operator approach can be seen in the next example where the sensor accuracy spatially varies.

Case II $\quad Q = 10^4,\ R = \sqrt{3}/x$

In this case, no measurement is available at x=0, and the accuracy of the measurement increases as x increases. The norm of Q/R is identical to the previous case, so the same expansion of the differential operator applies. In this case, the first order operator approximations to the optimal estimator gains are

$$\frac{P_3}{R} = \sqrt{\sqrt{3}\,\frac{Qx}{R}} + \ldots$$

$$\frac{P_1}{R} = \sqrt{2}\sqrt[4]{\sqrt{3}\,\frac{Qx}{R}} + \ldots \qquad (36)$$

Again, the feedback gains obtained via the operator approach are compared to those obtained via the discrete approximation (fig. 10).

By allowing R to be a function of x, it is possible to approximate the case of spatially discrete sensors by choosing appropriate continuous approximation functions for R(x).

Case III $\quad Q = 10^{-4},\ R = 1$

For Q/R small, or alternatively, for estimation of the component of the motion due to high frequency behavior, a different expansion of (33) gives:

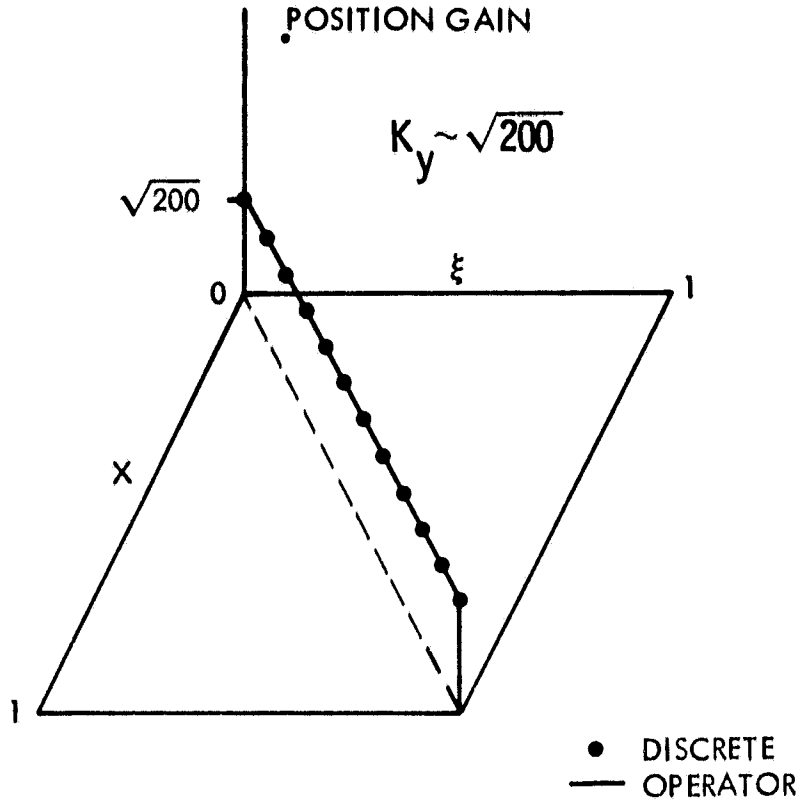

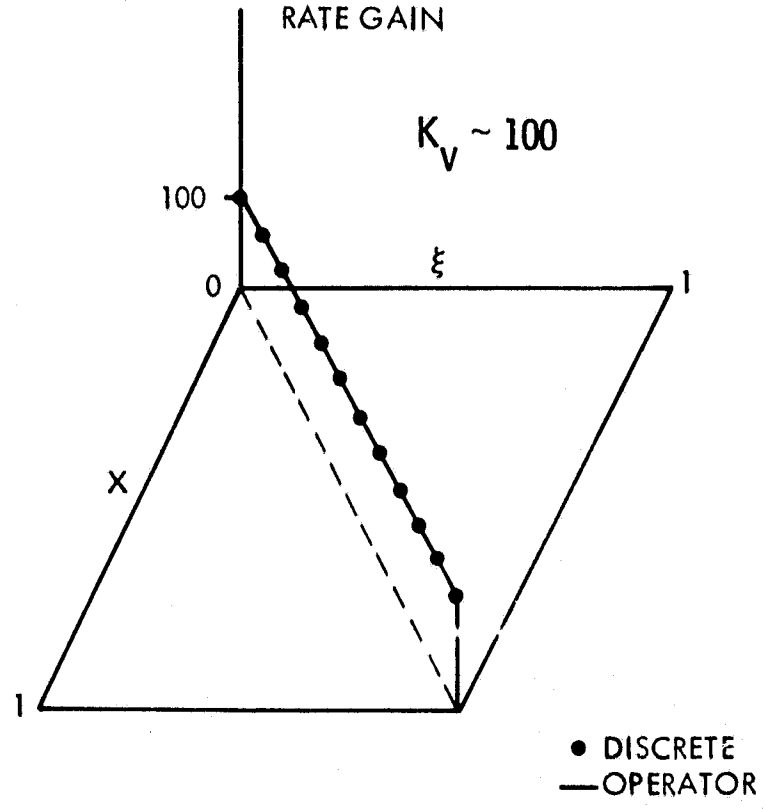

Figure 9. Operator vs. Discretized Control System Design Results (constant weight)

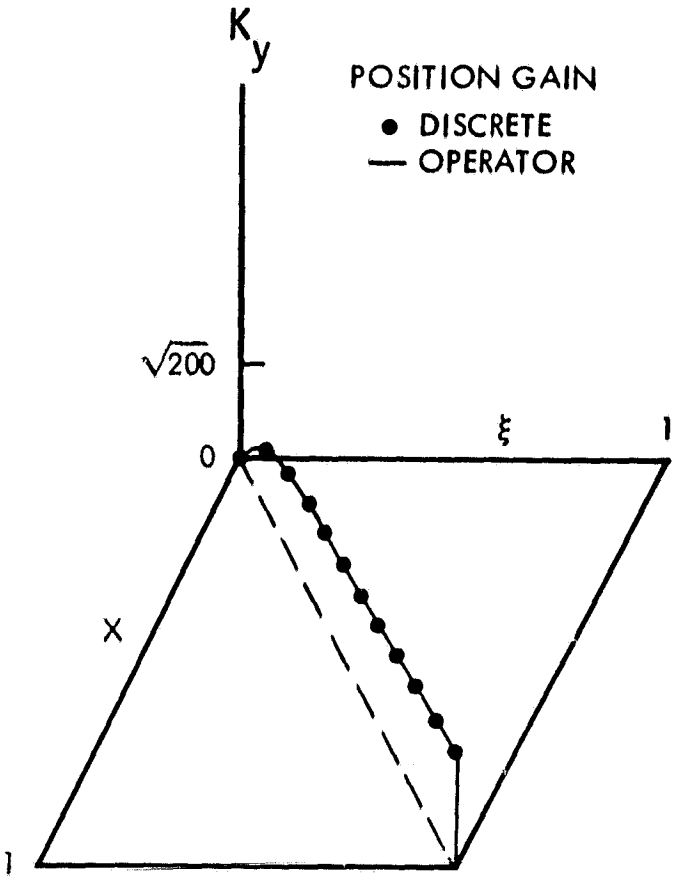

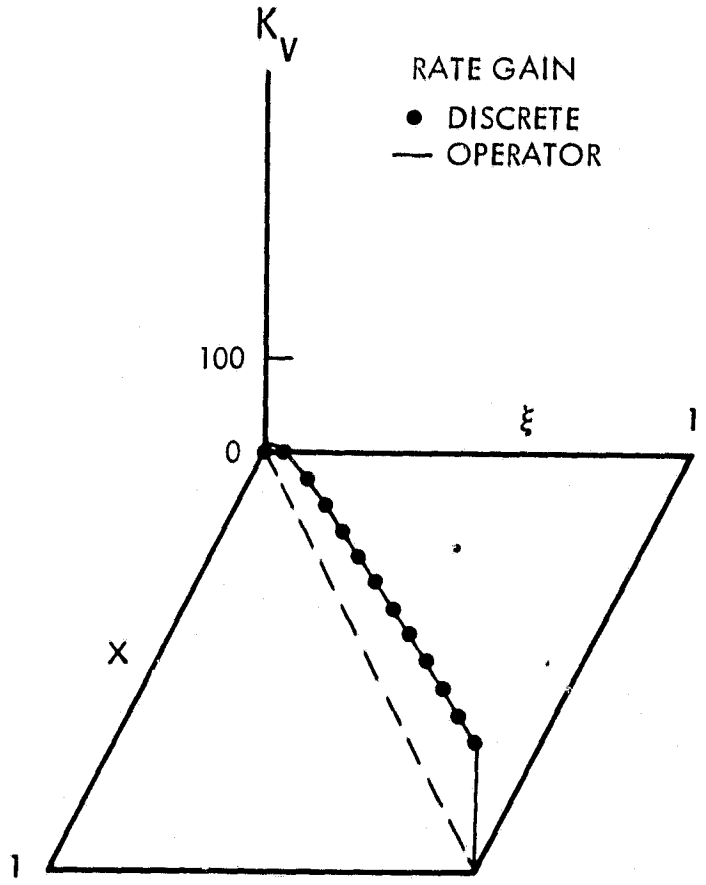

Figure 10. Operator vs. Discretized Control System Design Results (variable weight)

$$P_3/R = -\frac{Q/R}{2D^2} + \frac{(Q/R)^2}{8D^6}$$

$$P_1/R = \sqrt{\frac{Q}{R}}\ \sqrt{\frac{-1}{D}} + \ldots \tag{37}$$

As would be expected, for $Q/R = 0$, the steady state estimator gains are zero. For Q/R not equal to zero, the inverse powers of D must be interpreted as inverse operators. For the case of the flexible string, the inverse operator to D^2 that satisfies the boundary conditions is simply the integral operator whose kernel is the Green's function for the string, i.e.

$$\frac{1}{D^2}\ f = \int_0^1 g_1(x,\xi)\ f(\xi)\ d\xi \tag{38}$$

where

$$g_1(x,\xi) = \begin{cases} \xi(x-1) & x > \xi \\ x(\xi-1) & x < \xi \end{cases}$$

Note that $-1/D^2$ has a positive norm.

The analytical expression for the $\sqrt{-1}/D$ operator is somewhat more complex, and somewhat more interesting.

$$\frac{\sqrt{-1}}{D}\ f = \int_0^1 g_2(x,\xi)\ f(\xi)\ d\xi \tag{39}$$

where

$$g_2(x,\xi) = \frac{1}{\pi}\ \ln\ \left|\frac{\sin \pi(x+\xi)}{\sin \pi(x-\xi)}\right|$$

It should be noted that this operator satisfies the required boundary conditions at 0 and 1, but has the peculiarity of being infinite at $x=\xi$. At first, it might not seem reasonable that a particular point along the string could have an infinite weight contribution to the control law. In fact, this is not the case. The kernel does have an infinite value at $x=\xi$, but the fact that this is an integrable singularity, and that the kernel does appear under an integral, puts this feature in the proper perspective. It also explains why the gains computed using a discretized

system dynamics are not infinite valued at $x=\xi$, but instead are an average value over the discretization interval (fig. 11).

The Green's function and its square root yield control and estimator gains and appear naturally in the PDE formulation for controlling (damping) high frequency modes. These concepts can be extended to include general models based on FE by using the eigensystem expansion of the Green's function.

The Green's function can be expanded as

$$g_1(x,\xi) = \sum_{i=1}^{\infty} \frac{\phi_1(x)\ \phi_2(\xi)}{\lambda_i} \qquad (40)$$

and

$$g_2(x,\xi) = \sum_{i=1}^{\infty} \frac{\phi_i(x)\ \phi_i(\xi)}{\sqrt{\lambda_i}}$$

where the ϕ's and λ's are the normalized eigenfunctions and eigenvalues of the operator. For the case of an FE control design, the eigensystem analysis is usually performed as part of the structural analysis. The fact that these results can be directly used for control system design, as well, is a valuable new result.

The results obtained in this section are generally applicable to a wide range of PDE models, not just the string in tension. The general result can be summed up as follows.

Local estimation and control is optimal for the high gain, low frequency modes, where performance is required; and estimation and control based on the Green's function and its square root is optimal for the low gain, high frequency modes, where damping augmentation is required.

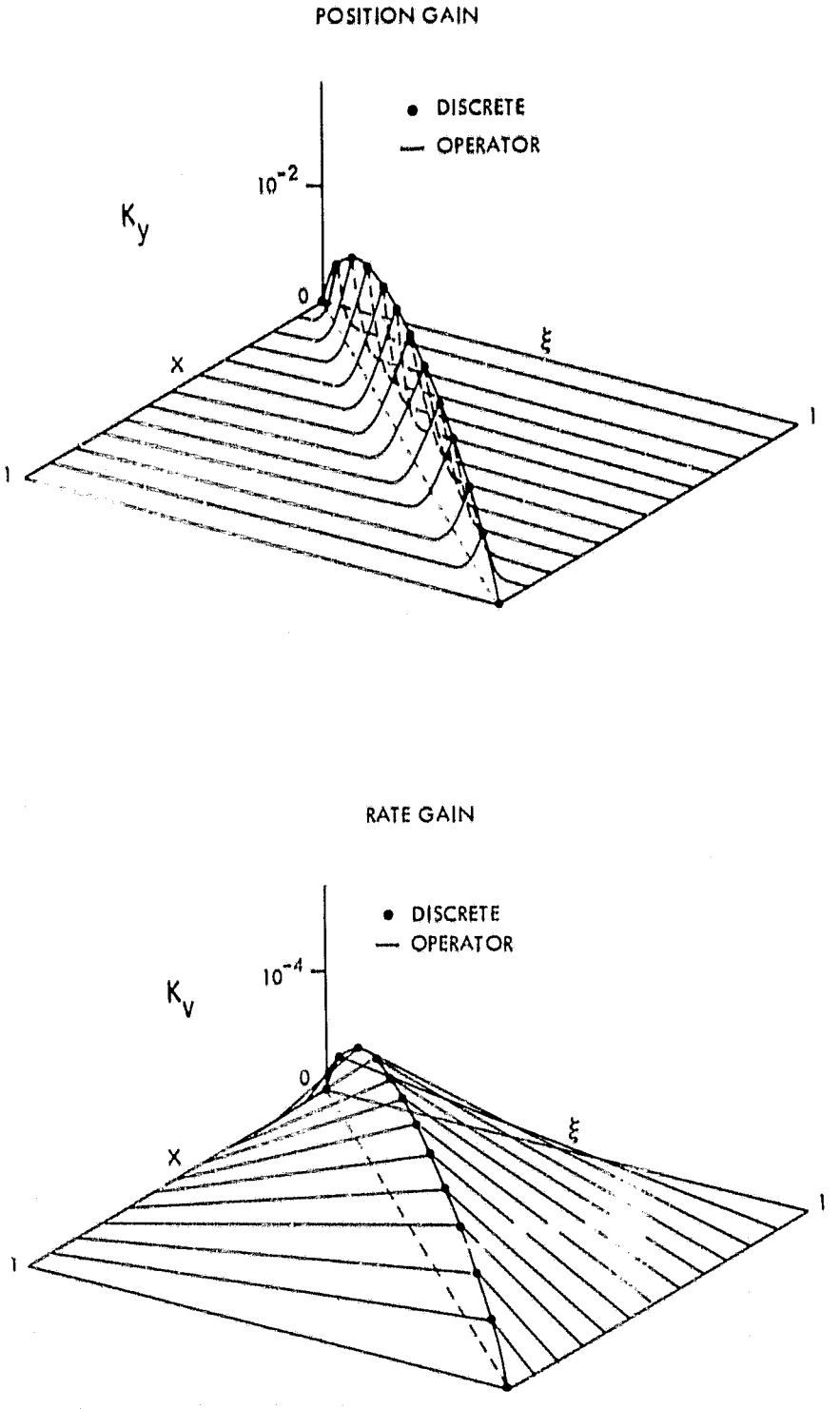

Figure 11. Operator vs. Discretized Control System Design Results (low gain)

Section 5

5.0 Shape Control

5.1 Introduction

Large, lightweight, flexible, space structures exhibit dynamic shape variations greater than those of any previous spacecraft. Whereas the shape varies continuously with changes in space and time, it must be estimated (controlled) by sensors (actuators) placed at discrete points along the structure.

The mixing of continuous and discrete mathematics can present or ease difficulty in the solution of control and estimation problems, depending on the method by which it is approached. The use of Green's functions to convert boundary value problems into integral equations provides a convenient treatment of these problems.

The Green's Function provides a solution to a nonhomogeneous ordinary or partial linear differential equation in terms of an integral operator which acts on the forcing function (the nonhomogeneous term). Comparison of solutions for different forcing functions becomes relatively easy. Furthermore, the expression of the solution in terms of the Green's function is especially convenient in the case of the spatially discrete functions found in large space structure control and estimation problems, since some integrals become finite sums.

The use of an integral operator rather than a differential one possesses additional advantages:

(1) The expression of a solution as an integral equation automatically incorporates the boundary conditions, which must be handled separately if the problem is stated as a differential equation.

(2) The integral operator is usually bounded and often completely continuous, whereas differential operators are unbounded. Thus results concerning eigenfunction expansions, solutions of nonhomogeneous equations, etc. are more easily obtained.

(3) Numerical approximations and variational techniques which include several other methods of solving problems with constraints are more easily applied to integral rather than differential equations.

5.2 The General Boundary Value Problem and Green's Function[14,15]

We first define a general boundary value problem and discuss the use of the Green's function in its solution. We then apply the technique to the solution of a general control problem and a general estimation problem for large space structures.

Consider a surface which occupies a simply connected region Ω and is bounded by the curve Γ.

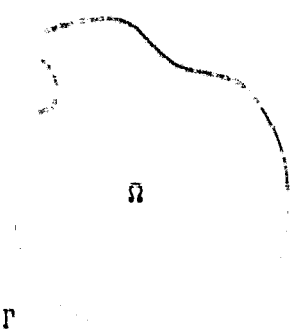

Assume the surface is acted on at each point $P\in\Omega$ by a force $f(P)$ and that the static deformation $u(P)$ of the surface satisfies the partial differential equation

$$Lu = f \tag{41}$$

where L is a linear partial differential operator, and also satisfies appropriate boundary conditions

$$B_i(u) = 0, \qquad 1 \leq i \leq N, \quad \text{for } P\in\Gamma . \tag{42}$$

Assume the boundary conditions (42) are such that the operator L is self-adjoint. That is

$$(Lu,v) = (u,Lv) \tag{43}$$

for any pair of functions (u,v) in an appropriate class which satisfy the boundary conditions (42). The inner product (u,v) is defined to be the integral

$$(u,v) = \int_\Omega u(Q)\, v(Q)\, dQ \,. \tag{44}$$

We also assume, for convenience, that the homogeneous system

$$Lv = 0, \quad B_i(v) = 0 \,, \qquad 1 \le i \le N \tag{45}$$

has only the trivial solution. This is equivalent to the assumption that the system has no rigid body modes.

Thus, the general boundary value problem is the system (41-42) together with the assumptions (43-45).

The Green's function $g(P,Q)$ associated with the boundary value problem (41-42) satisfies

$$Lg(P,Q) = \delta(P-Q) \tag{46a}$$

$$B_i(g) = 0 \,, \quad 1 \le i \le N \,, \quad \text{for } P \in \Gamma \,. \tag{46b}$$

It represents the response at the point P to a unit impulsive force at Q. Since L is self-adjoint $(u,Lg) = (Lu,g)$, which provides the solution to the boundary value problem (41-42):

$$u(P) = \int_\Omega u(Q)\, \delta(P-Q)\, dQ = \int_\Omega g(P,Q)\, f(Q)\, dQ \,. \tag{47}$$

Remark 1. The Green's function is the kernel of the compact integral operator K such that

$$Kf = \int_\Omega g(P,Q)\, f(Q)\, dQ \,. \tag{48}$$

K is clearly the inverse of the operator L, where defined on the range of L, since $KLu = Kf = u$ and $LKf = Lu = f$.

Remark 2. The solution of (46a) is called a fundamental solution. The equation (46a) is satisfied in a distributional rather than a pointwise sense. That is

$$(Lg,\phi) = (g,L^*\phi) = \phi(\xi) \tag{49}$$

for all test functions ϕ. (A test function is an infinitely differentiable function defined on a domain which has compact support.)

There are some additional requirements for a solution in the case that (45) has non-trivial solutions, that is, the physical system possesses rigid body modes. In this case, (41) has no solution unless the "consistency condition"

$$(f, v) = 0$$

is satisfied for every v(Q) which is a solution of (45).

The consistency condition becomes reasonable when we consider that seeking a solution to (41) for any function f in some space is equivalent to seeking the inverse of the operator L in that space. If the null space of L is zero (i.e. the solution of (45) is only the trivial solution) then L is one to one and its inverse may be defined. If (46) has non-trivial solutions, L is not one to one and L^{-1} may be defined, if at all, not uniquely on the range of L. The consistency condition guarantees that f has no component in the null space of L, hence (with a little more work) that it is in the range of L.

If we approach the determination of the Green's function as we did for the beam with simply supported endpoints then the attempt to solve the BVP in (46) results in an immediate stumbling block. This system has a solution only if

$$(\delta(P-Q), \quad v(Q)) = 0 \tag{50}$$

for every solution v(Q) of (48). But, the delta function, in general, has components in the space of solutions to the homogeneous problem, so instead we seek the modified Green's function which satisfies

$$L\, g(P,Q) = \delta(P-Q) - \sum_i u_i(P)\, u_i(Q) \tag{51}$$

where the $u_i(P)$ are the normalized, non-trivial solutions of (45).

We have subtracted the offending components of $\delta(P-Q)$ which lie in the nullspace of L. A solution to this system does exist.

If the Green's function is known, the solution (47) of the boundary value problem is known. If $g(P,Q)$ is not known (47) is an expression of the solution in terms of a compact operator which incorporates the boundary conditions. Approximate solutions may be computed from the eigenfunction expansions

$$g(P,Q) = \sum_{k=1}^{\infty} \frac{1}{\lambda_k} \phi_k(P)\ \phi_k(Q) \tag{52}$$

and

$$Kf = \int_\Omega g(P,Q)\ f(Q)\ dQ = \sum_{k=1}^{\infty} \frac{1}{\lambda_k} \phi_k(P)\ (\phi_k,f) \tag{53}$$

where λ_k are the non-zero eigenvalues and ϕ_k are the corresponding normalized eigenfunctions of (41-42), which satisfy $L\phi_k = \lambda_k\ \phi_k$ and $B_i(\phi_k) = 0$, $1 \leq i \leq N$.

Substitution of expression (52) for f in (53) yields the following relation which will also be useful:

$$\int_\Omega g(P_i,Q)\ g(Q,P_j)\ dQ = \sum_{k=1}^{\infty} \frac{1}{\lambda_k^2} \phi_k(P_i)\ \phi_k(P_j)\ . \tag{54}$$

Alternatively, other numerical methods may be applied with greater convenience to (47) then to the original boundary value problem (41-42), because of the superior properties of integral over differential operators.

5.3 The General Shape Control Problem

In this section we define a general control problem and a general estimation problem corresponding to large space structures. We then solve these problems using the results of the last section. In the next section we will give specific examples of problems and their solutions.

The control/sensor mechanisms for large space structures will probably be located at discrete points P_i, $1 \leq i \leq m$, along the structure, rather than continuously. Thus the general dynamical model for the control problem is

$$Lu = \sum_{i=1}^{m} f_j\ \delta(P-P_i) \tag{55}$$

$$B_j(u) = 0\ , \quad 1 \leq j \leq N \tag{56}$$

where $u(P)$ is the shape, L is a linear differential operator as before, f_i is a force to be applied at the position P_i, and (56) denotes an appropriate set of boundary conditions.

Let $\psi(Q)$ be the desired shape of the space structure, and define the quadratic criterion

$$J(F,u) = \frac{1}{2} \sum_{i=1}^{m} f_i^2 \, q_i + \frac{1}{2} \int_\Omega (\psi(Q) - u(Q))^2 \, dQ \tag{57}$$

as a measure of performance. The constants q_i are arbitrary weights and $F = (f_1 \ldots f_m)^T$.

The control problem is to determine the vector of forces F^* which together with the corresponding solution u^* of (55-56) minimizes J over all admissible sets (F,u).

The solution of (55-56) is given by

$$\begin{aligned} u(P) &= \int_\Omega g(P,Q) \, [\sum_{i=1}^{m} f_i \, \delta(Q-P_i)] \, dQ \\ &= \sum_{i=1}^{m} f_i \, g(P,P_i) \end{aligned} \tag{58}$$

where $g(P,Q)$ satisfies (46). Substitution of (58) into the criterion (57) yields the criterion

$$\hat{J}(F) = \frac{1}{2} \sum_{i=1}^{m} f_i^2 \, q_i + \frac{1}{2} \int_\Omega (\psi(Q) - \sum_{i=1}^{m} f_i g(Q,P_i))^2 \, dQ \, . \tag{59}$$

The constrained optimization problem (55-57) has become the simpler problem of minimizing a function of m unknown constants without constraints. Solving simultaneously the equations

$$\frac{\partial \hat{J}}{\partial f_i} = 0 \qquad 1 \leq i \leq m \, , \tag{60}$$

we are lead to the following necessary condition for an optimal solution $F^* = (f_1^* \ldots f_m^*)^T$:

$$(\bar{Q} + A) \, F^* = B \tag{61}$$

The m x m matrices $\bar{Q}$ and A have coefficients

$$\bar{Q}_{ij} = q_i \, \delta(i-j)$$

$$A_{ij} = \int_\Omega g(P_i,Q) \; g(P_j,Q) \; dQ \tag{62}$$

and the m dimensional vector B has coefficients

$$B_i = \int_\Omega g(P_i,Q) \; \psi(Q) \; dQ \; . \tag{63}$$

Once the optimal forces are determined, the optimal shape u* is given by (58).

It is interesting to note at this point that the necessary indications for the shape control problem require only that $\bar{Q}$ be positive semidefinite, since A is positive definite. That is to say, in contrast with the full state optimal controllers in the time domain, placing a zero weighting on a particular control will not result in unbounded control forces. A simple example will serve as the explanation of this phenomena.

Consider an elastic beam pinned at both ends with a control force located at the center. If it is desired to bend the beam into any shape which is not symmetric with respect to the applied force, no amount of control force will accomplish the task exactly. That is to say, even with a zero weighting on the cost of control, a bounded value of control force will come closest to producing the desired shape.

5.4 The General Shape Estimation Problem

For the estimation problem we assume the shape u(P) satisfies the boundary value problem

$$Lu = f \; , \; B_i(u) = 0 \; , \qquad 1 \leq i \leq N \; , \tag{64}$$

where f(P) is an unknown function representing disturbances or errors in the model. Sensors placed at the positions P_i, $1 \leq i \leq m$, yield the observations

$$y_i = u(P_i) + v_i \tag{65}$$

where v_i is an unknown constant representing inaccuracy in the observation at P_i. Let $V = (v_1 \ldots v_m)$. We define the performance criterion

$$J(V,f) = \frac{1}{2} \sum_{i=1}^{m} v_i^2 \, q_i + \frac{1}{2} \int_\Omega f^2(Q) \, dQ$$

$$= \frac{1}{2} \sum_{i=1}^{m} (y_i - u(P_i))^2 \, q_i + \frac{1}{2} \int_\Omega f^2(Q) \, dQ \, . \tag{66}$$

The estimation problem is to determine the pair (u*,f*) which jointly satisfy '64-65) and minimize the criterion (66) over all admissible pairs (u,f).

The solution to (63) is given by

$$u(P) = \int_\Omega g(P,Q) \, f(Q) \, dQ \tag{67}$$

where g(P,Q) again satisfies (46). Thus

$$v_i = y_i - \int_\Omega g(P_i,Q) \, f(Q) \, dQ \tag{68}$$

We substitute (68) into the criterion (66), which produces the criterion

$$\hat{J}(f) = \frac{1}{2} \sum_{i=1}^{m} (y_i - \int_\Omega g(P_i,Q) f(Q) dQ)^2 \, q_i + \frac{1}{2} \int_\Omega f^2(Q) \, dQ \, . \tag{69}$$

The problem is now to minimize the functional $\hat{J}$ without constraints. A necessary condition for a minimum of $\hat{J}$ at f* is that the differential

$$\partial J(f^*,h) = 0 = \sum_{i=1}^{m} q_i (y_i - \int_\Omega g(P_i,(Q) f^*(Q) dQ)(- \int_\Omega g(P_i,Q) h(Q) dq)$$

$$+ \int_\Omega f^*(Q) h(Q) \, dQ \tag{70}$$

for all admissible variation h. Thus it may be concluded that

$$f^*(P) = \sum_{i=1}^{m} q_i \, g(P,P_i)(y_i - u^*(P_i)) \, . \tag{71}$$

Substitution of this relation into (25) yields the optimal shape estimate

$$u^*(P) = \sum_{i=1}^{m} [q_i (y_i - u^*(P_i)) \int_\Omega g(P,Q) \, g(P_i,Q) dQ] \, . \tag{72}$$

Note that u*(x) is expressed in terms of the unknown discrete shape estimates $u^*(P_i)$. Let

$$X = (u^*(P_1) \ . \ . \ . \ u^* \, (P_m))^T \tag{73}$$

and

$$Y = (y_1 \ \cdots \ y_m)^T \tag{74}$$

Evaluation of (72) at $x = x_j$, $j = 1, \ldots, m$ yields the following necessary condition for the vector x:

$$(I + A\bar{Q})\ X = A\bar{Q}Y \ . \tag{75}$$

where A and $\bar{Q}$ are the matrices of coefficients (62).

Once the vector X has been determined the optimal shape estimate is given by (72).

In the case the Green's function is not precisely known, or is unwieldy, approximate solutions may be obtained using the eigenfunction expansion (54) for the coefficients A_{ij}

5.5 Examples of Static Shape Estimation and Control

Case I Shape Control for a Simply Supported Beam

Consider the problem of controlling the static deflection of an elastic beam of length ℓ (fig. 12). Define a coordinate system such that the x-axis passes through the endpoints of the beam, with one end at the origin and the other at $x = \ell$. Suppose control is to be implemented by means of transverse forces f_i at positions x_i, $1 \leq i \leq m$, where $0 < x_1 < x_2 \ \ . \ . \ . < x_m < \ell$.

At each point $x \in [0,\ell]$ denote the deflection by u(x). Assuming no net tensile force on a cross-section, the shape of the beam is governed by the differential equation

$$\frac{d^4u}{dx^4} = \sum_{i=1}^{m} f_i\ \delta(x-x_i) \tag{76}$$

The ends of the beam satisfy the boundary conditions

$$u(0) = u''(0) = 0 \quad u(\ell) = u''(\ell) = 0 \tag{77}$$

Let $\psi(x)$ be the desired shape of the beam. As a measure of performance we define the criterion

$$J(u,F) = \frac{1}{2} \sum_{i=1}^{m} f_i^2 q_i + \frac{1}{2} \int_0^{\ell} (u(x)-\psi(x))^2\ dx \tag{78}$$

where F is the vector of forces $(f_1 \ \cdots \ f_m)^T$ and q_i are non-negative constant weights whose values are optional.

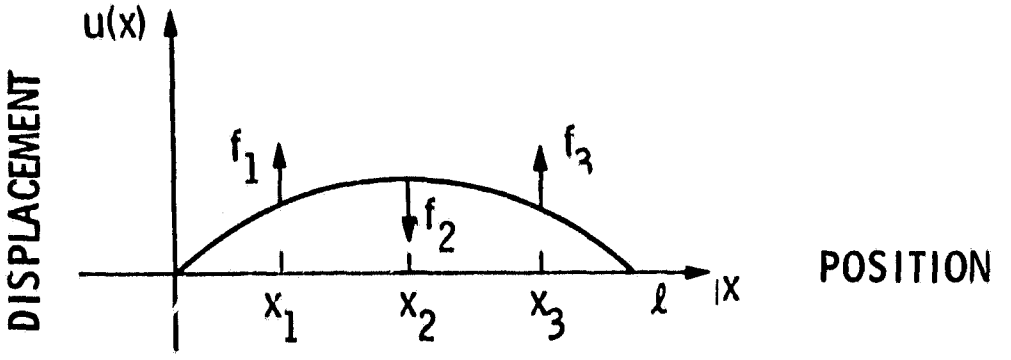

Figure 12. The Simply Supported Beam

The object is to determine the set of forces f_i^* which together with the solution $u^*(x)$ of (76) minimizes (78) over all possible pairs (u,F).

The solution of (76) is given by

$$u(x) = \sum_{i=1}^{m} g(x,x_i) f_i \tag{79}$$

where $g(x,\xi)$ is the Green's function associated with (76,77) which satisfies

$$\frac{d^4 g(x,\xi)}{dx^4} = \delta(x-\xi) \tag{80}$$

$$g(0,\xi) = g''(0,\xi) = 0 \quad g(\ell,\xi) = g''(\ell,\xi) = 0 \ . \tag{81}$$

The Green's function represents the natural response of the beam to a unit impulsive force at $X = \xi$. The existence and uniqueness of the solution to (80,81) follows from the fact that the associated homogeneous system

$$\frac{d^4 v}{dx^4} = 0 \quad v(0) = v''(0) = 0 \quad v(\ell) = v''(\ell) = 0 \tag{82}$$

has the only trivial solution. The solution of (80,81) is

$$g(x,\xi) = \begin{cases} \frac{(\xi-\ell)x}{6\ell}\,(x^2-2\ell\xi+\xi^2) & 0 \le x \le \xi \\ \frac{(x-\ell)\xi}{6\ell}\,(x^2-2\ell x+\xi^2) & \xi \le x \le \ell \end{cases} \tag{83}$$

Figure 13 displays the Green's function which corresponds to impulsive forces at positions $\xi = n\,(\frac{\ell}{8})$, $n = 1, \ldots, 7$.

The solution of the control problem follows. Substitution of the solution (79) into the criterion (78) yields

$$\hat{J}(F) = \frac{1}{2} \sum_{i=1}^{m} f_i^2 q_i + \frac{1}{2} \int_0^{\ell} \Big(\sum_{i=1}^{m} g(x,x_i) f_i - \psi(x) \Big)^2 \, dx \tag{84}$$

The problem of minimizing the criterion (78) subject to the constraints (76-77) has become the problem of minimizing a function of m unknown constants without constraints. A necessary condition for J to have a minimum at F* is

$$\frac{\partial \hat{J}}{\partial f_i}(F^*) = 0 \qquad 1 \le i \le m \tag{85}$$

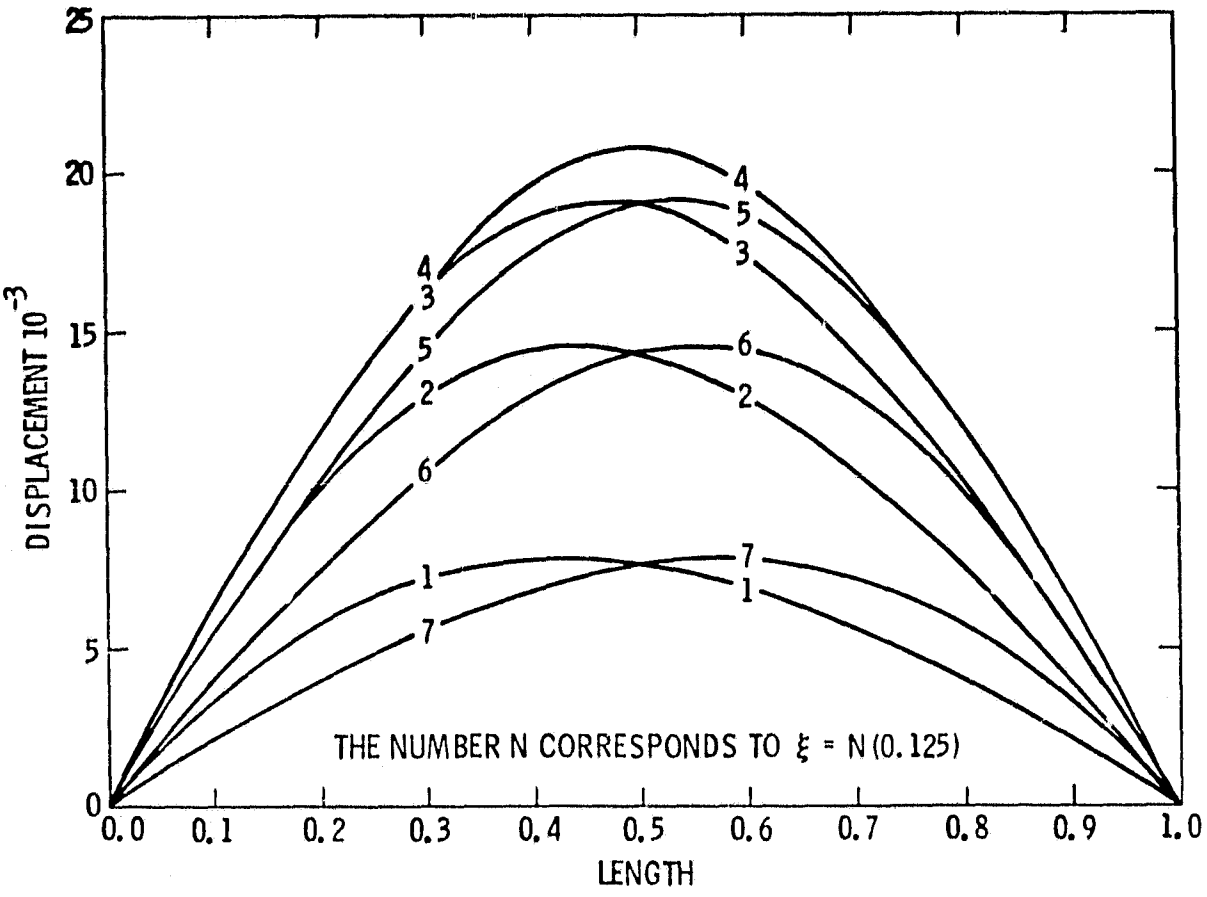

Figure 13. The Green's Function for the Simply Supported Beam

This condition becomes

$$f_i q_i + \sum_{i=1}^{m} f_k \left(\int_0^{\ell} g(x,x_i) g(x,x_k) dx \right) = \int_0^{\ell} \psi(x) g(x,x_i)\ dx \ . \tag{86}$$

If we define

$$a_{ij} = \int_0^{\ell} g(x,x_i) g(x,x_j)\ dx, \qquad 1 \leq i,\ j \leq m \ , \tag{87}$$

and

$$b_i = \int_0^{\ell} \psi(x)\ g(x,x_i)\ dx, \qquad 1 \leq i \leq m \ , \tag{88}$$

then the necessary condition for a minimum of J at F* is that F* satisfy

$$(I + AQ)F = A\ Q\ B \tag{89}$$

where Q is the m x m diagonal matrix

$$Q = \begin{pmatrix} q_1 & & \\ & \ddots & \\ & & q_m \end{pmatrix} \tag{90}$$

A is the m x m matrix with coefficients (87), and B is the m dimensional vector with coefficients (88).

The shape control algorithm for the simply supported beam

(1) Compute the constants a_{ij} and b_j defined by (87-88). Define Q,A,B.

(2) Solve (89) to get F*.

(3) The optimal shape $u^*(x) = \sum_{i=1}^{m} f_i^* g(x,x_i)$.

Figure (14) displays the optimal shape vs. the desired shape $\psi(x) = \sin \frac{2\pi x}{\ell}$, the second mode of the system (76,77), for two actuators at 1/4ℓ and 3/4ℓ.

Case II. The Control Problem for the Pinned-Free Beam

A modification of the control algorithm is necessary if the system has rigid body modes, as is the case with the pinned-free beam.

The beam with one pinned and one free end point satisfies the differential equation (76) with boundary conditions

$$u(0) = u''(0) = 0 \quad u''(\ell) = u'''(\ell) = 0. \tag{91}$$

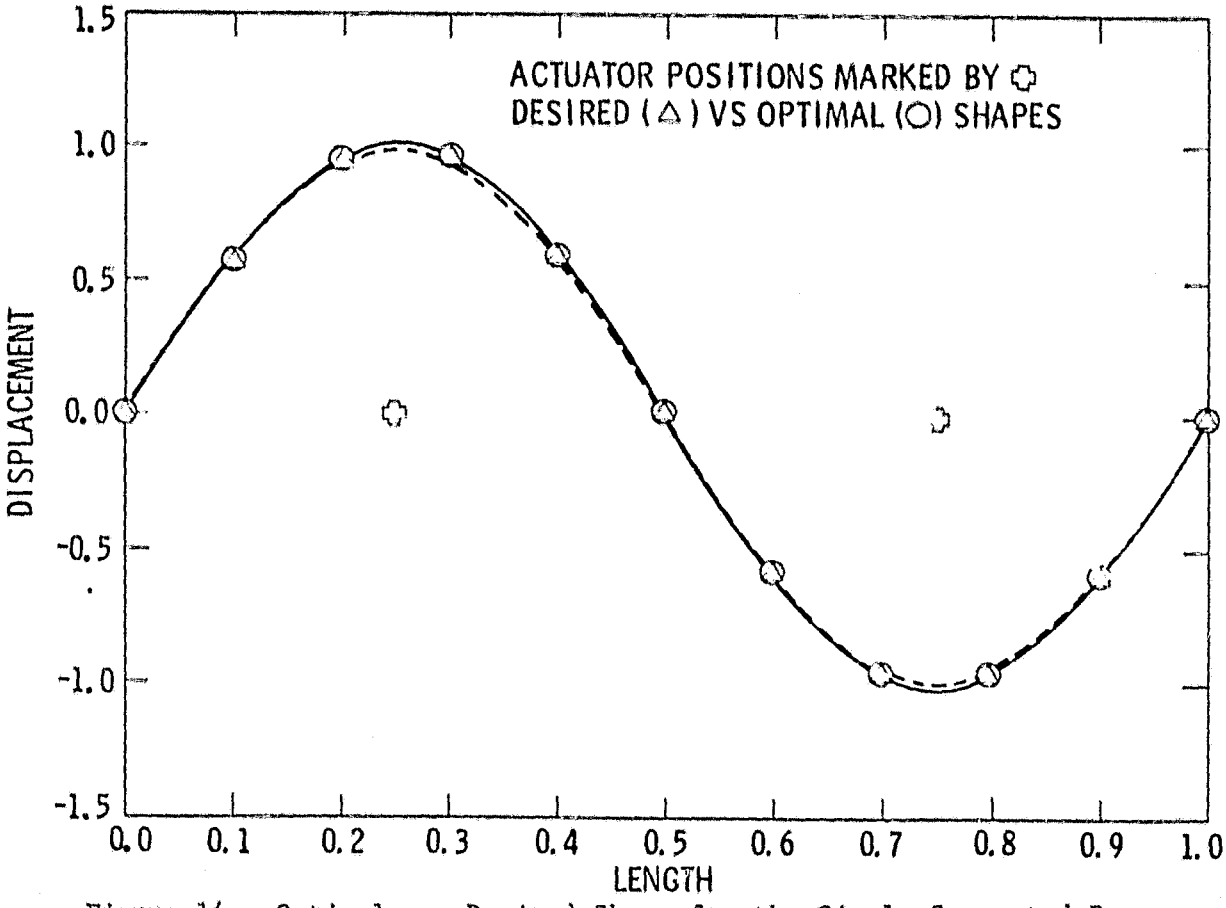

Figure 14. Optimal vs. Desired Shape for the Simply Supported Beam

We will again use the performance criterion (78). The object is to determine the set of forces $\{f_i\}$ which together with the solution $u(x)$ of (76,91) minimizes (78) over all possible pairs $(\{f_i\}, u)$

The system (76,91) has the rigid body mode $u_1(x) = \sqrt{\frac{3}{\ell^3}}\, x$ (normalized). Physically this means the beam can have a non-zero slope or tilt as a rigid body. Mathematically it means that the corresponding homogeneous system

$$\frac{d^4v}{dx^4} = 0 \qquad v(0) = v''(0) = 0 \qquad v''(\ell) = v'''(\ell) = 0 \tag{92}$$

has the non-trivial solution $u_1(x)$. Thus the system (76,91) has a solution only if the inner product

$$\left(\sum_{i=1}^{m} f_i\, \delta(x-x_i),\ u_1\right) = \sqrt{\frac{3}{\ell^3}} \sum_{i=1}^{m} f_i x_i = 0\ . \tag{93}$$

The additional constraint (93) must be added to the problem of determining the optimal control forces.

A solution to (80) with pinned-free boundary conditions does not exist because the inner product $(\delta(x-\xi),\ u_1)$ is not zero. The "modified" Green's function which is appropriate to the system (76,91) satisfies

$$\frac{d^4 g_m(x,\xi)}{dx^4} = \delta(x-\xi) - \frac{3}{\ell^3}\, x\xi \tag{94}$$

$$g_m(0,\xi) = g_m''(0,\xi) = 0 \qquad g_m''(\ell,\xi) = g_m'''(\ell,\xi) = 0 \tag{95}$$

We make the additional requirement that $g_m(x,\xi)$ have no component in the subspace spanned by the rigid body modes.

$$(g_m(x,\xi), u_1) = \sqrt{\frac{3}{\ell^3}} \int_0^{\ell} g_m(x,\xi)\, x\, dx = 0 \tag{96}$$

The modified Green's function which satisfies (94-96) is given by

$$g_m(x,\xi) = x\xi\left(\frac{33\ell}{140} + \frac{\xi^2+x^2}{4\ell} - \frac{\xi^4+x^4}{40\ell^3}\right) - \begin{cases} \frac{\xi^3 x}{2} + \frac{x^3}{6} & 0 \le x \le \xi \\ \frac{x^2\xi}{2} + \frac{\xi^3}{6} & \xi \le x \le \ell\ . \end{cases} \tag{97}$$

Condition (96) guarantees that $g_m(x,\xi)$ is symmetric and of minimum norm among all solutions of (94,95).

The Green's function (97) represents the response of the pinned-free beam to one of a set of unit impulsive forces which satisfy (93). Figure 15 displays the Green's function for impulsive forces at positions n $(\frac{\ell}{8})$, n = 1,...,7.

The solution of (76, 91, 93) is given by

$$v(x) = \sum_{i=1}^{m} f_i \, g_m(x,x_i) \tag{98}$$

We solve (93) for f_1 in terms of the other forces and substitute that expression together with (96) into the criterion (78), which results in

$$\hat{J}(\hat{F}) = \frac{q_1}{2}\left(\sum_{i=2}^{m} \frac{x_i}{x_1} f_1\right)^2 + \frac{1}{2}\sum_{i=2}^{m} f_i^2 \, q_i$$
$$+ \frac{1}{2}\int_0^{\ell}\left(\sum_{i=2}^{m} f_i\left(g_m(x,x_i) - \frac{x_i}{x_1} g(x,x_i)\right) - \psi(x)\right)^2 dx \tag{99}$$

where $\hat{F}$ is the vector $(f_2 \ldots f_m)^T$.

Again, the optimization problem is reduced to one of minimizing a function of unknown constants.

The necessary condition for a minimum at F* is

$$\frac{\partial J}{\partial f_i}(\hat{F}^*) = 0 \qquad 2 \leq i \leq m \, . \tag{100}$$

The conditions (100) result in the following algorithm.

(1) Compute the m dimensional vector B and m x m matrix A whose coordinates are

$$b_i = \int_0^{\ell} g_m(x,x_i) \, \psi(x) \, dx \tag{101}$$

$$a_{ij} = \int_0^{\ell} g_m(x,x_i) \, g_m(x,x_j) \, dx \, . \tag{102}$$

(2) Compute the (m-1) dimensional vector B and (m-1) x (m-1) matrix A whose coordinates are

$$\hat{b}_i = b_{i+1} - \frac{x_{i+1}}{x_1} b_1$$

$$\hat{a}_{ij} = (q_1 + a_{11}) \frac{x_{i+1}x_{j+1}}{x_1^2} \tag{103}$$

$$+ a_{i+1,j+1} - a_{1,i+1} \frac{x_{j+1}}{x_1} - a_{1,j+1} \frac{x_{i+1}}{x_1} \tag{104}$$

Let $\hat{Q}$ be the (m-1) x (m-1) diagonal matrix

$$\hat{Q} = \begin{pmatrix} q_2 & & \\ & \ddots & \\ & & q_m \end{pmatrix} \tag{105}$$

(3) The vector $\hat{F}^*$ of optimal forces satisfies

$$(\hat{Q} + \hat{A})\hat{F}^* = \hat{B} \ . \tag{106}$$

The optimal force f_1^* is found from (93).

(4) The optimal shape $u^*(x) = \sum_{i=1}^{m} f_i^* g_m(x,x_i)$.

Since the optimal shape u^* is a linear combination of Green's functions which satisfy (96), it will have no component in the subspace of the rigid body mode. If the desired shape $\psi(x)$ does have such a component, that is if (ψ,u_1) is not zero, the optimal shape will approximate the shape

$$\psi(x) - (\psi,u_1)\ u_1(x) \ . \tag{107}$$

That is, it will approximate the desired shape minus its component in the subspace spanned by $u_1(x)$.

As an example, Figure 16 displays the desired shape $\psi(x) = \ell x - x^2$, the shape which approximates $\frac{3}{4}\ \ell x - x^2$, and the optimal shape plus the missing rigid body mode component $\frac{1}{4}\ \ell x$.

Those components of the desired shape in the subspace spanned by rigid body modes must be added by the attitude control system. A shape control system constrained to satisfy the boundary conditions cannot affect these components.

Case IV. The Shape Estimation Problem

To illustrate the shape estimation algorithm we consider a simply supported beam of length ℓ and unknown shape $u(x)$, which satisfies

$$\frac{d^4u}{dx^4} = f(x) \quad \text{on} \quad 0 \leq x \leq \ell, \tag{108}$$

and

$$u(0) = u''(0) = 0 \qquad u(\ell) = u''(\ell) = 0$$

The function $f(x)$ represents minor model inaccuracies or random disturbances acting on the beam.

Assume sensors at positions x_i, $0 < x_1 < \ldots < x_m < \ell$, produce observations

$$z_i = u(x_i) + V_i , \qquad 1 \leq i \leq m . \tag{109}$$

As a measure of the accuracy of shape estimates we define the criterion

$$J(f,u) = \frac{1}{2} \sum_{i=1}^{m} (z_i - u(x_i))^2 q_i + \frac{1}{2} \int_0^{\ell} f^2(x)\, dx . \tag{110}$$

The object is to determine the function f^* which together with the solution u^* of (108) minimizes (110) over all possible pairs (f,u).

The solution of (108) is given by

$$u(x) = \int_0^{\ell} g(x,\xi)\, f(\xi)\, d\xi \tag{111}$$

where $g(x,\xi)$ is the Green's function (83). We substitute (117) into the criterion (110); resulting in the criterion

$$\hat{J}(f) = \frac{1}{2} \sum_{i=1}^{m} q_i \left(z_i - \int_0^{\ell} g(x_i,\xi) f(\xi) d\xi\right)^2 + \frac{1}{2} \int_0^{\ell} f(\xi)^2\, d\xi. \tag{112}$$

The estimation problem has reduced to one of minimizing (112) without constraints. A necessary condition for J to have a minimum at f^* is that

the Frechet d' ferential

$$\partial\hat{J}(f,h) = \sum_{i=1}^{m} q_i\Big(z_i - \int_0^{\ell} g(x_i,\xi) f^*(\xi)\, d\xi\Big)$$

$$\Big(- \int_0^{\ell} g(x_i,\xi) h(\xi) d\xi\Big) + \int_0^{\ell} f^*(\xi) h(\xi) d\xi = 0$$

for all admissible variations h. This implies

$$f^*(\xi) = \sum_{i=1}^{m} q_i g(x_i,\xi)(z_i - u^*(x_i)) \ . \tag{113}$$

Then

$$u^*(x) = \sum_{i=1}^{m} q_i (z_i - u^*(x_i)) \int_0^{\ell} g(x,\xi) g(x_i,\xi)\, d\xi. \tag{114}$$

Let

$$X = (u^*(x_1) \ \ldots \ u^*(x_m))^Y$$

and

$$Z = (z_1 \ \ldots \ z_m)^T \ .$$

Evaluation of (114) at $x = x_j$ and regrouping of terms yield the following necessary condition for the vector X:

$$(I + AQ)\ X = AQZ \tag{115}$$

where A is the matrix of coefficients (87), Q is the diagonal matrix (90).

The shape estimation algorithm.

(1) Compute the elements of the matrix A given by (87), and define X,Q,Z.

(2) Solve the system (115) for the vector X.

(3) The optimal error estimates are given by (41) and $v_i = z_i - u^*(x_i)$, $1 \le i \le m$.

(4) The optimal shape estimate is given by (114).

This algorithm is equally valid for the static beam with other boundary conditions, provided the appropriate Green's function is used.

Figure 17 displays the optimal shape estimate versus the actual shape

$$\sin\left(\frac{\pi x}{\ell}\right) + \frac{1}{2}\sin\left(\frac{2\pi x}{\ell}\right) \ ,$$

for three exact observations at $\frac{1}{4}\,\ell$, $\frac{1}{2}\,\ell$, and $\frac{3}{4}\,\ell$.

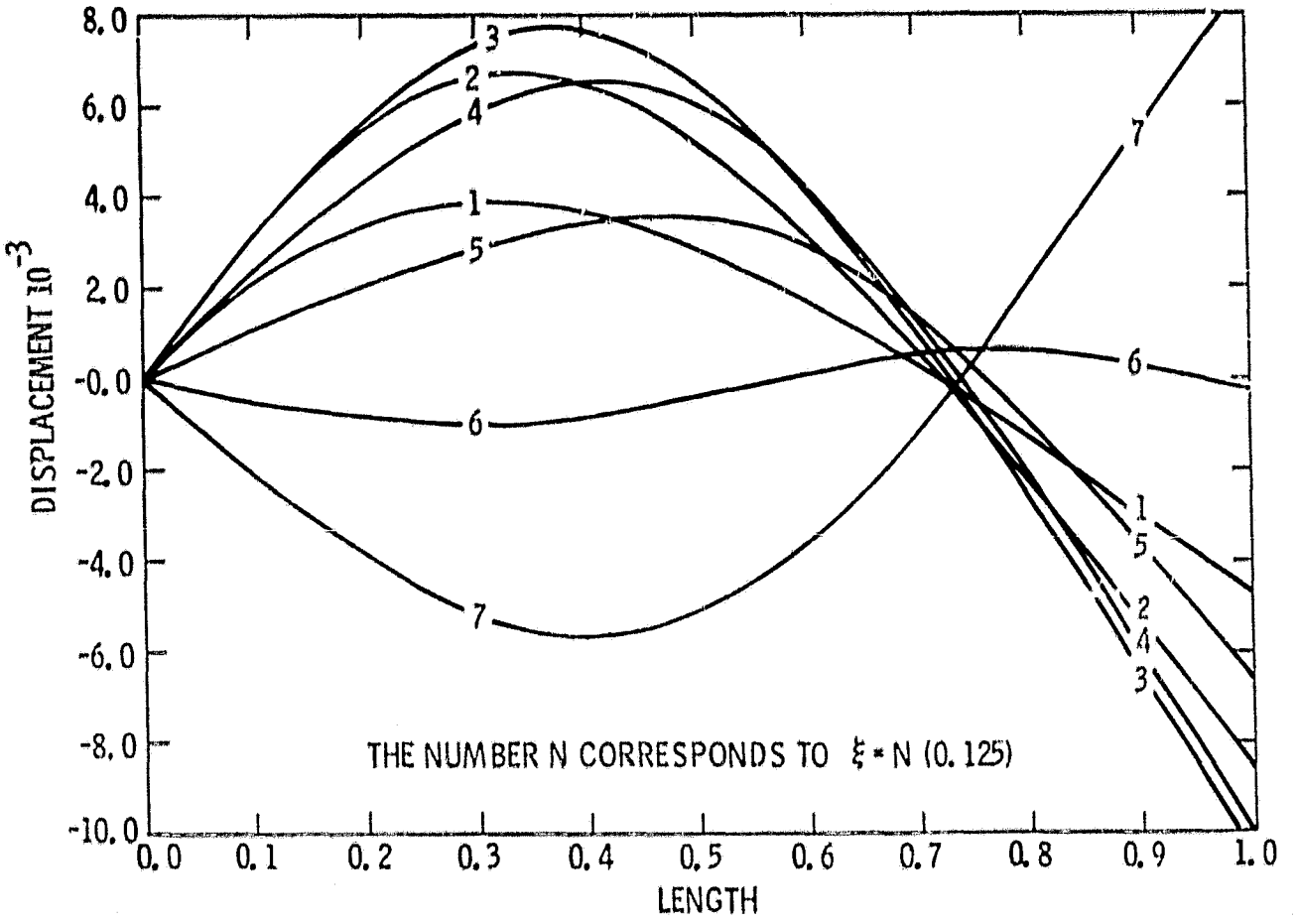

Figure 15. Green's Function for the Pinned-Free Beam

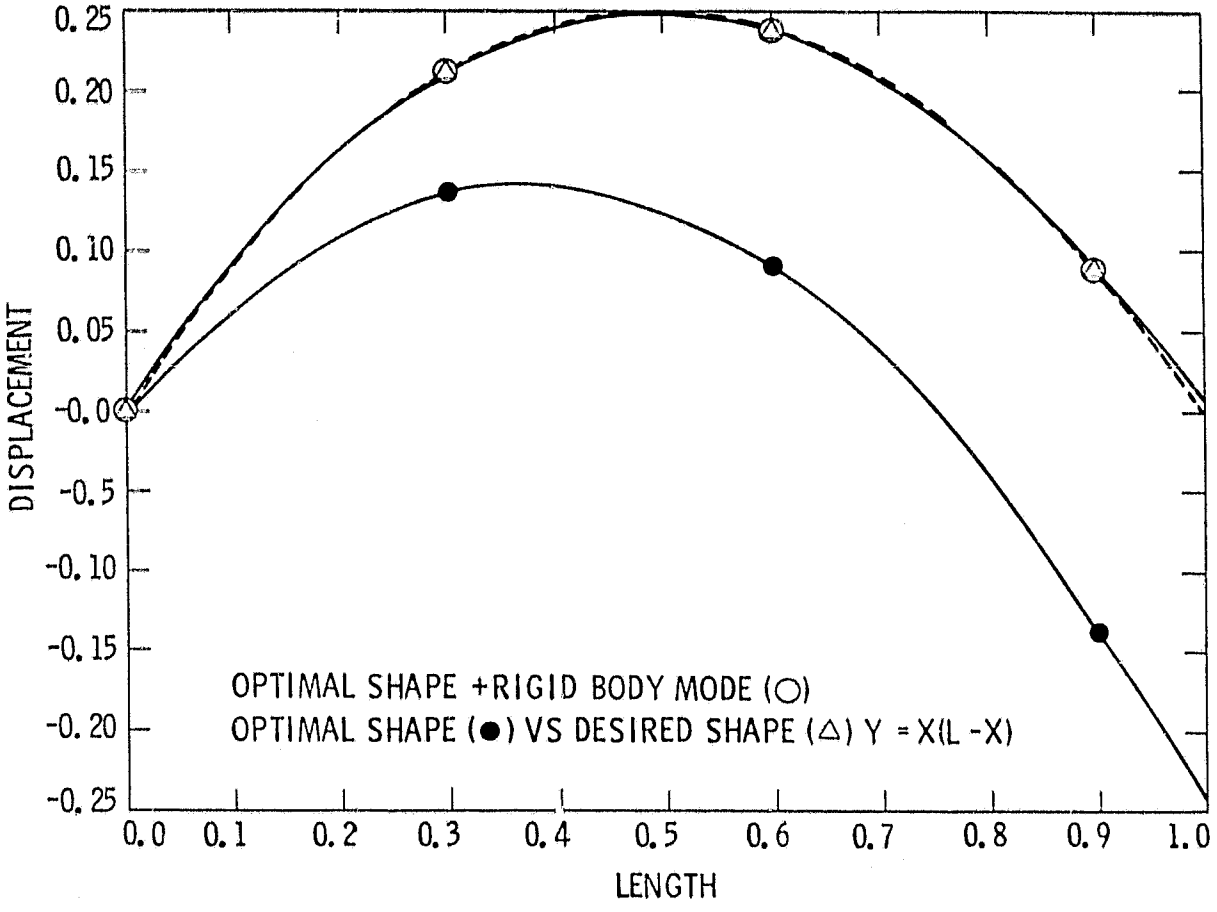

Figure 16. Shape Estimation with Rigid Body Modes

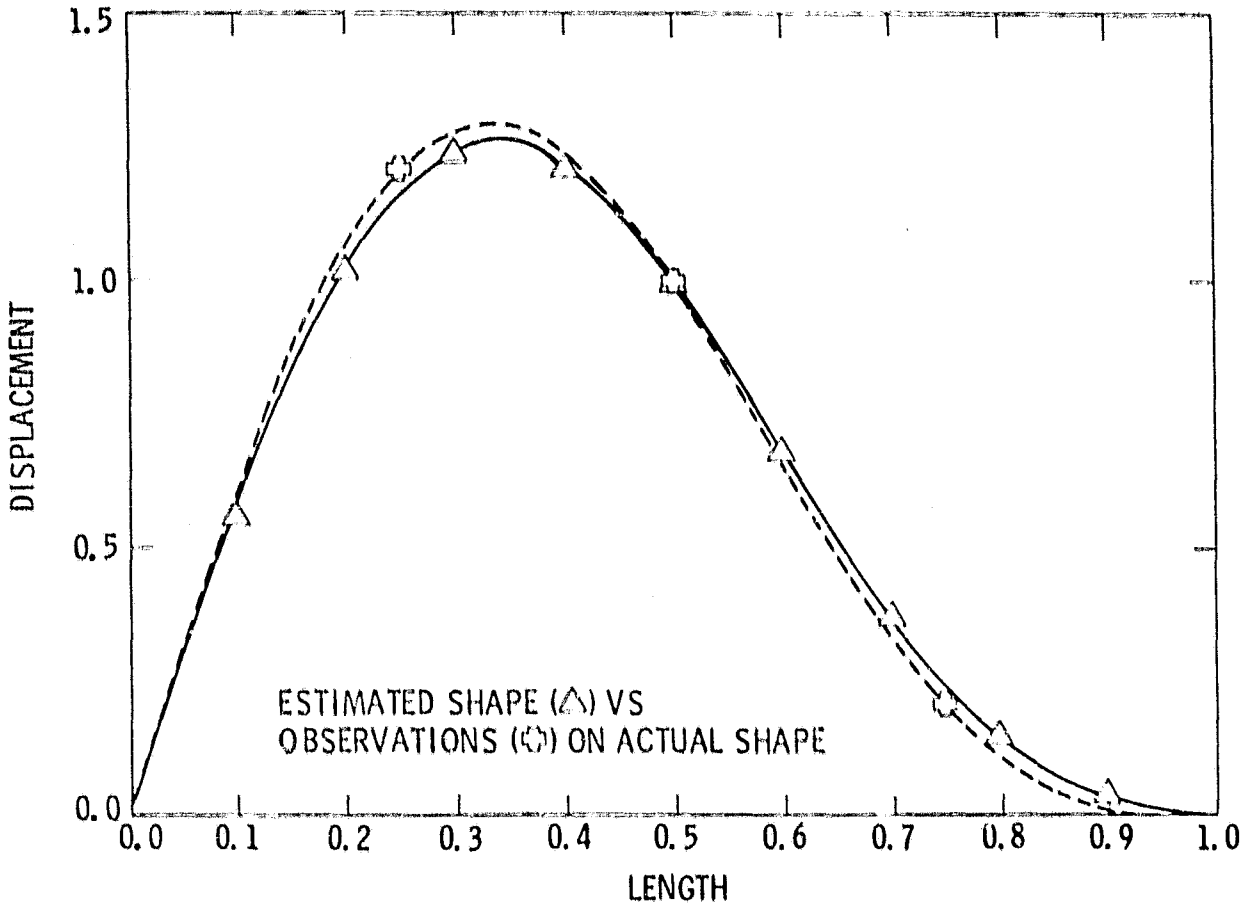

Figure 17. Shape Estimation Results

5.6 Approximations for Shape Estimation and Control

The following approximations are particularly desirable when the system models are more complicated so that the Green's functions are difficult to compute analytically. They are based on the assumption that the Green's function is symmetric and of minimum norm, which follows if the boundary value problem is self-adjoint.

$$a_{ij} = \int_0^{\ell} g_m(x,x_i)g_m(x,x_j)dx = \sum_{k=1}^{\infty} \frac{1}{\lambda_k^2} \phi_k(x_i)\phi_k(x_j)$$
$$b_i = \int_0^{\ell} \psi(x)g(x,x_i)dx = \sum_{k=1}^{\infty} \frac{1}{\lambda} \phi_k(x_i)(\phi_k,\psi) \qquad (116)$$

where x_i's are the actuator (or sensor) positions, λ_k's are the non-zero eigenvalues, and the ϕ_k's are the corresponding normalized eigenfunctions of the associated boundary value problems.

Simulations of approximations based on the first term in each of these expansions generated approximate optimal shapes which were visually indistinguishable from the optimal shapes, and numerically accurate to the third or fourth significant figure.

Section 6

6.0 Experimental Verification of Distributed Control Concepts

6.1 Introduction

The previous sections of this document have contained new developments in the theory of the control of large space structures. In some cases, computer simulations of these new developments have been performed to verify the analytical results. One vital phase of this research and development program still remains to be presented, experimental verification. Laboratory verifications of the analysis and computer simulation are required to fill the gap prior to the final, flight project, stage of the large structure work.

An experiment employing a pinned-free flexible beam has been constructed to demonstrate and verify several facets of the control of flexible structures. The desired features of the experiment are to demonstrate active shape control, active dynamic control, adaptive control, various control law design approaches, and associated hardware requirements and mechanization difficulties. This section contains the analytical work performed in support of the facility development, the final design specifications, control law synthesis, and some preliminary results.

The flexible beam was chosen for this experiment for being a simple, continuous structure with many of the dynamic characteristics that are representative of general large space structures, including, infinitely many vibration modes, a rigid body mode, and many, "low" frequency vibration modes.

The selection of the flexible beam also resulted in some minor limitations. The flexible beam does not have repeated eigenvalues, however, by orthogonality of the corresponding eigenvectors, these modes may be distinguished spatially, if not by frequency domain methods. Secondly, totally free boundary-conditions are not possible in a ground based experiment. Two beam support configurations which replace the rigid body mode with a low frequency pendulum mode were considered as alternatives and are shown in figure 18.

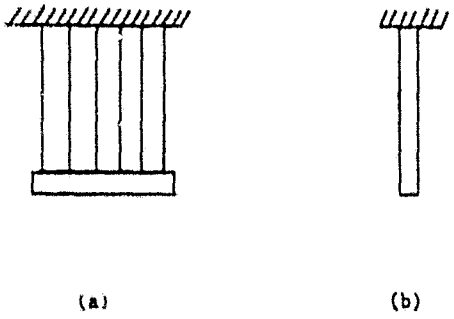

Figure 18. Beam Support Configurations

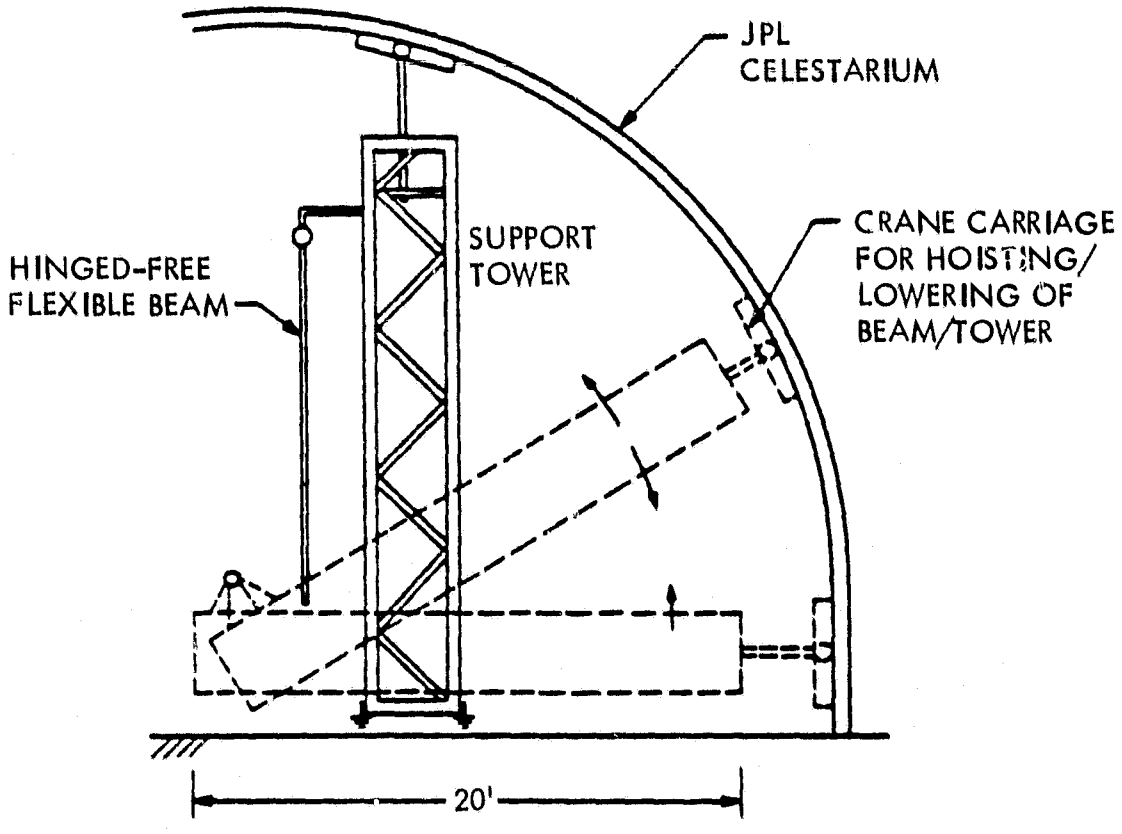

Figure 19. Beam Support Structure

Figure 18a shows the beam supported by several cables in the horizontal direction and figure 18b shows the beam hanging vertically from a pinned support. Although the configuration in figure 18a more closely approximates the totally free boundary conditions, the complexity of distributing the weight of the beam uniformly and the difficulty with constraining the unwanted degrees of freedom in 18a resulted in selection of pinned-free hanging beam of 1b as the final configuration.

One further compromise had to be made in the sensing/actuation phase of this experiment. A totally free space structure is constrained to sense with respect to (and react against) itself, or inertial space. Because the major objectives of this experiment are to demonstrate control technology, and not sensor/actuator technology, sensing and actuation of the beam are both performed with respect to an external frame.

6.2 Dynamic Analysis of Flexible Beam Facility

A schematic of the beam and its support structure (tower) as they are being erected is shown in figure 19. The tower is constructed of aluminum angles and is twenty feet tall, two feet deep in the stiff direction and one foot deep in the compliant direction. The weight of the tower is two hundred pounds. With the sensor/actuator mounting brackets (figure 20), beam, sensors, actuators, and electronics, the total weight is about three hundred pounds.

Shake tests were performed on the tower to determine its resonances, and if they might interact with the control of the flexible beam. The results are given in order of increasing frequency in Table II.

Table II Tower Resonances

Frequency (hz)	Mode	Direction
6	cantilever	compliant
10	cantilever	stiff
27	pinned-free	compliant
35	pinned-free	stiff
45	free-free	compliant
63	free-free	stiff

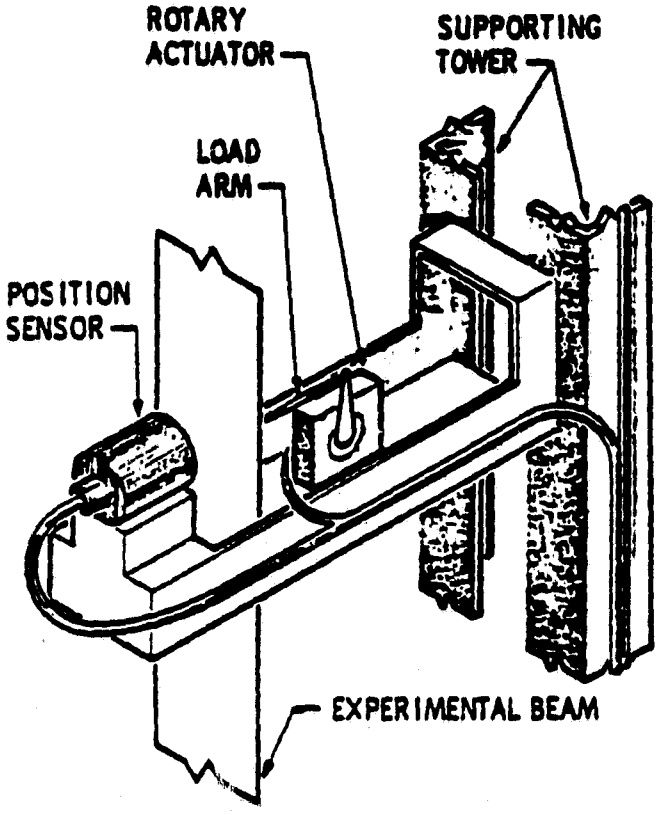

Figure 20. Sensor/Actuator Mounting Bracket

For the final configuration, only the natural frequencies in the stiff direction are of interest because there is very little coupling between the perpendicular directions.

A schematic of the sensor/actuator mounting bracket is shown in figure 20. Either the sensor, or actuator, or both may be mounted on a single bracket, and the brackets may be mounted at any of the stations located at six inch intervals along the beam.

A dynamic model of the hanging, pinned free beam is required for control system design. Two modeling approaches will be examined here; first, an analytical approach, and, second, a finite element model.

Temporarily setting aside the effects of the beam being in tension due to gravity, the partial differential equation of motion for the elastic beam with constant mass and stiffness per unit length and the appropriate boundary conditions are

$$\rho \frac{\partial^2 y}{\partial t^2} + EI \frac{\partial^4 y}{\partial x^4} = f \tag{117}$$

$$y(0,t) = 0 \quad \frac{\partial^2 y}{\partial x^2}(L,t) = 0$$

$$\frac{\partial^2 y}{\partial x^2}(0,t) = 0 \quad \frac{\partial^3 y}{\partial x^3}(L,t) = 0$$

It is straightforward to show by assuming an eigenvector decomposition of the solution that the eigenvalues and normalized eigenvectors are

$$\phi_o(\xi) = \sqrt{\frac{3}{L}}\,\xi \qquad \omega_o = 0$$

$$\phi_n(\xi) = \sqrt{\frac{\frac{2}{L}\cosh^2\lambda_n \cos^2\lambda_n}{\cosh^2\lambda_n - \cos^2\lambda_n}}\left[\frac{\sinh\lambda_n\xi}{\cosh\lambda_n} + \frac{\sin\lambda_n\xi}{\cos\lambda_n}\right] \tag{118}$$

where

$$\omega_n^2 = \frac{EI\lambda_n^4}{\rho L^4}$$

and

$$\tanh\lambda_n = \tan\lambda_n$$

and

$$\xi = \frac{x}{L}$$

Using an asymptotic approximation (good for $n \geq 1$) for (118)

$$\phi_o(\xi) = \sqrt{3}\,\xi \qquad \omega_o = 0$$

$$\phi_n(\xi) = \frac{1}{\sqrt{L}} \left[\frac{\sin\lambda_n\xi}{\cosh\lambda_n} + \frac{\sin\lambda_n\xi}{\cos\lambda_n} \right] \qquad \lambda_n \simeq \frac{(4n+1)\pi}{4} \qquad (119)$$

$$n = 1,2,3,\ldots$$

The dynamic equations for the modal amplitudes, q_n, become

$$\ddot{q}_n + \omega_n^2 q_n = \int_0^1 \frac{\phi_n(\xi) f(\xi) d\xi}{\rho} \triangleq f_n \qquad n = 0,1,2\ldots \qquad (120)$$

For the specific case that $f(\xi,t) = F(t)\,\delta(\xi_o)$, i.e., a spatially concentrated force applied at $\xi = \xi_o$,

$$f_n = \frac{F}{M}\,\phi_n(\xi_o) \qquad (121)$$

A graph of the first four mode shapes is shown in figure 21.

The rigid body motion of figure 21 is a zero frequency eigenvalue. Of course, for the pinned-free beam hanging under the influence of gravity, no such mode exists. Rather than being a zero frequency, rigid body mode, the actual dynamics is a low frequency, pendulum-like behavior. In fact, gravity interacts with all of the modes to some degree. To determine which behavior (tension or elastic) dominates the various modes, an independent dynamic analysis of a hanging free string will be performed.

The partial differential equation of motion for a hanging string, with its boundary conditions is

$$\rho \frac{\partial^2 y}{\partial t^2} = \frac{\partial}{\partial x}\left(\rho g x \frac{\partial y}{\partial x} \right) \qquad (122)$$

$$y\ (0) \text{ finite}$$

$$y\ (L) = 0$$

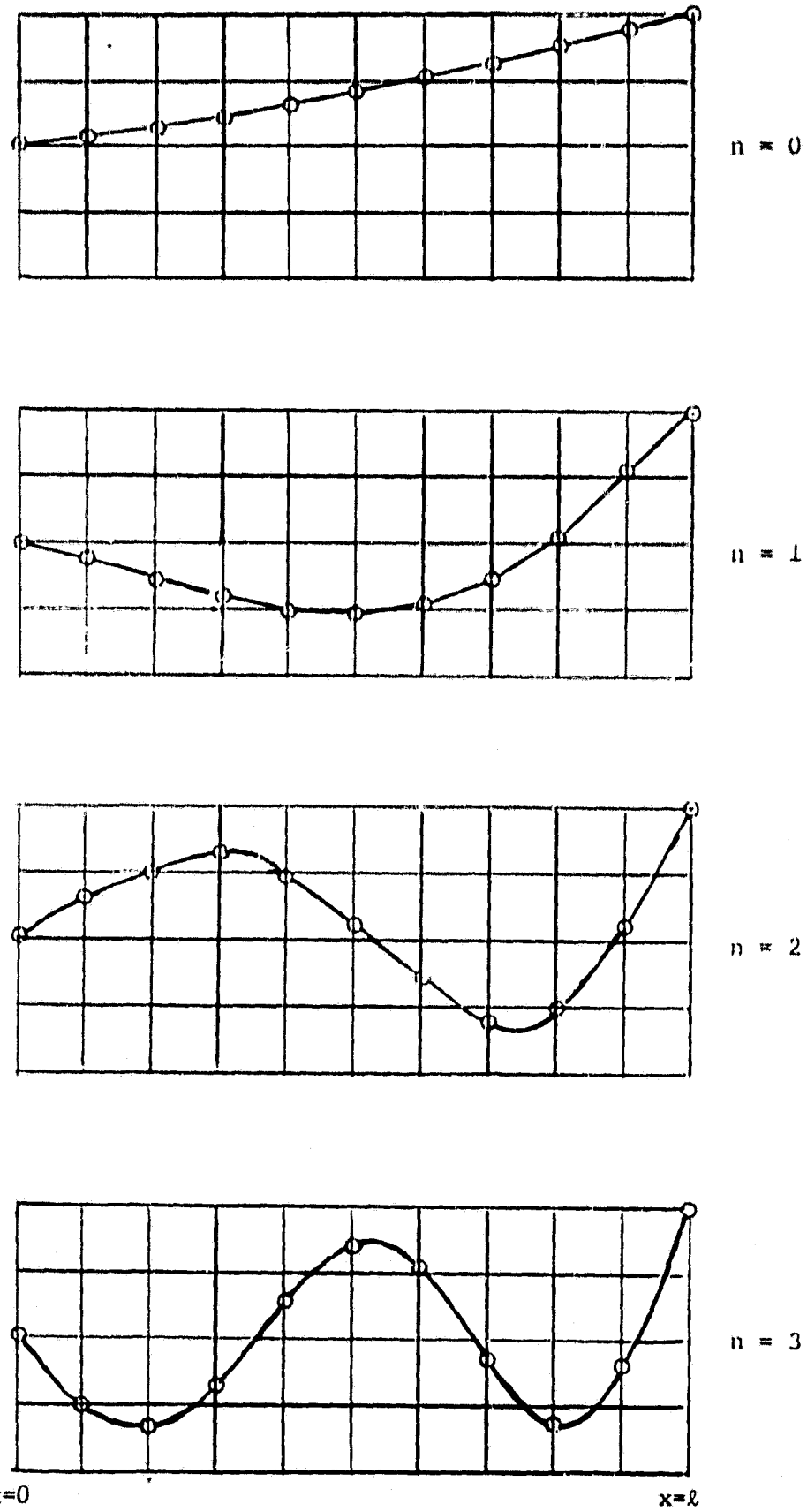

Figure 21. Beam Mode Shapes

The solution to (122) is given by

$$\phi_n = J_o\ (\omega_n \sqrt{\frac{4x}{g}})$$

where

$$J_o\ (2\ \omega_n \sqrt{\frac{L'}{g}}) = 0\ . \tag{123}$$

Again, an asymptotic approximation to the eigenvalues can be obtained

$$\omega_n^2 \approx \frac{g}{2L'} \frac{(n - 1/4)^2\ \pi^2}{2}$$

If the true mode shapes of the exact system are obtained from 124

$$\rho \frac{\partial^2 y}{\partial t^2} + EI \frac{\partial^4 y}{\partial x^4} - \rho\ g \frac{\partial}{\partial x} (L-x) \frac{\partial y}{\partial x} = f \tag{124}$$

it can be shown that the squares of the exact eigenvalues are approximately the sum of the squares of the string and the beam frequencies with the largest error occurring when the two frequencies are equal.

Using the experimentally obtained beam parameters appearing in Table III, the approximate modal frequencies and the experimentally determined modal frequencies can be compared. These results are contained in Table IV.

Since the exact analytical solution to the differential equation of motion is not known, a discretized, finite element model is developed. The beam is divided into N segments as shown in figure 22. The displacement and slope at the ends of each segment are specified as coordinates. Mass and stiffness matrices can be defined for each element, and these assembled to create overall mass and stiffness matrices for the system. The differential equation of motion is thereby replaced by a matrix eigenproblem, and arbitrary accuracy can be obtained by considering smaller divisions of the beam.

The stiffness matrix K for the finite element shown in figure 23 is defined by

$$U = 1/2 x^T K x \tag{125}$$

where U is the potential energy of the segment and

$$x^T = (x_1, x_2, x_3, x_4) \tag{126}$$

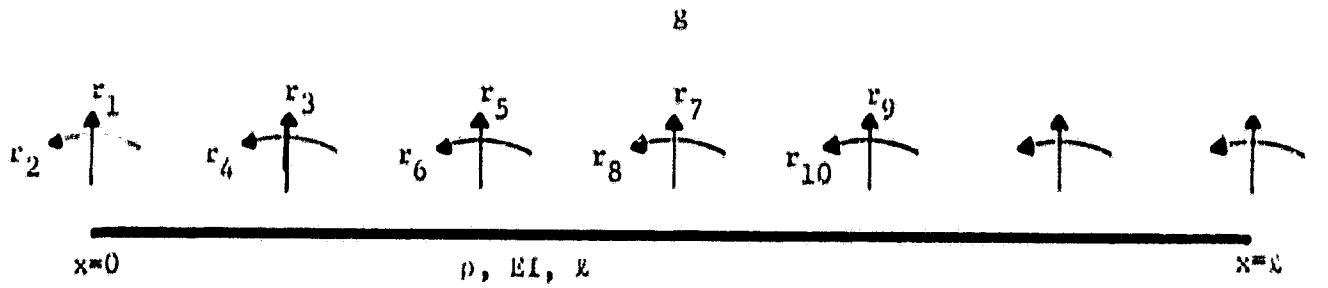

Figure 22. Finite Element Beam Model

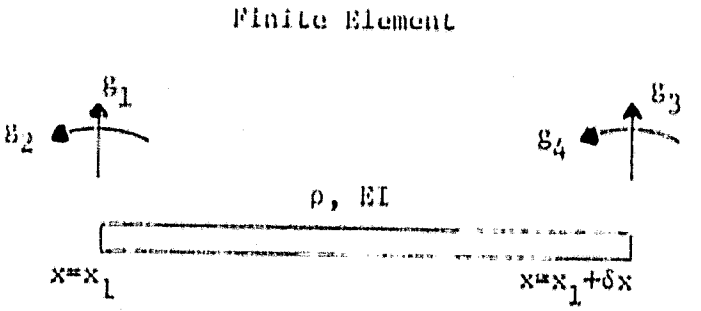

Figure 23. A Single Finite Element

gives the nodal displacements and slopes. Analytically U is given by

$$U = 1/2 \int_{x_1}^{x_1+\delta x} (EIy''^2 + \rho g(\ell - x)y'^2)\, dx$$

Substituting

$$z = \left(\frac{\rho g}{EI}\right)^{1/3} \ell\left(1 - \frac{x}{\ell}\right) \tag{127}$$

we obtain

$$U = \frac{-\rho g}{2} \int_{z_1}^{z_1+\delta z} (y''^2 + zy'^2)\, dz \tag{128}$$

where

$$z_1 = \left(\frac{\rho g}{EI}\right)^{1/3} \ell\left(1 - \frac{x_1}{\ell}\right) \tag{129}$$

and

$$\delta z = -\left(\frac{\rho g}{EI}\right)^{1/3} \delta x \tag{130}$$

The displacement y(z) of the finite element is chosen to minimize the potential energy U of the element. This is equivalent to assuming that the shape of the element is unaffected by dynamic loading.

Equating a variation of U to zero and integrating by parts, we obtain

$$y'''' - \frac{\delta}{\delta z}(zy') = 0 \tag{131}$$

whose solution is

$$y(z) = \alpha_0\phi_0(z) + \alpha_1\phi_1(z) + \alpha_2\phi_2(z) + \alpha_3\phi_3(z) \tag{132}$$

where the α_i's are constants and the ϕ_i's are linearly independent solutions of (131). Though the analytical solution to (131) is known in terms of Bessel functions of fractional order, it is more convenient to define the functions ϕ_i as infinite series. The choice used in this analysis is

$$\phi_0(z) = 1 \tag{133}$$

$$\phi_1(z) = (z - z_1) + \frac{(z - z_1)^4}{4!} + \ldots$$

$$\phi_2(z) = \frac{(z - z_1)^2}{2!} + \frac{z_1(z - z_1)^4}{4!} + \ldots$$

$$\phi_3(z) = \frac{(z - z_1)^3}{3!} + z_1 \frac{(z - z_1)^5}{5!} + \ldots$$

with coefficients of $(z - z_1)$ determined by the recursion relation

$$a_{n+3} = \frac{n a_n}{(n+1)(n+2)(n+3)} + \frac{z_1 a_{n+1}}{(n+2)(n+3)}$$

$$n = 1,2,3,\ldots \tag{134}$$

The functions ϕ_i are expanded about $z = z_1$ to ensure rapid convergence of the series.

Similar series expansions for the derivatives of ϕ_i are easily derived. Of course, in practice the series are truncated after a finite number of terms, once convergence has been determined.

Equation (132) can be written in matrix form as

$$y(z) = \phi^T \alpha \tag{135}$$

where

$$\phi^T = (\phi_0(z), \phi_1(z), \phi_2(z), \phi_3(z)) \tag{136}$$

$$\alpha^T = (\alpha_0, \alpha_1, \alpha_2, \alpha_3)$$

Furthermore, α can be related to q. Writing

$$q^T = (q_1, q_2, q_3, q_4) \tag{137}$$

$$= (y(x_1), \dot{y}(x_1), y(x_1 + \delta x), \dot{y}(x_1 + \delta x))$$

and substituting (135) into (137), we obtain

$$q = A\alpha \tag{138}$$

where the matrix A is given by

$$A = \begin{bmatrix} \phi(x_1)^T \\ \phi^1(x_1)^T \\ \phi(x_1 + \delta x)^T \\ \phi^1(x_1 + \delta x)^T \end{bmatrix} \tag{139}$$

Equations (138) can be rewritten as

$$\alpha = Bq \tag{140}$$

with

$$B = A^{-1}$$

Substituting (140) into (135), and that in turn into (128), we obtain

$$U = \frac{-\rho g}{2} q^T B^T \int_{z_1}^{z_1+\delta z} (\phi'' \phi''^T + z\phi' \phi'^T)\, dz B q \,. \tag{141}$$

Identifying terms with equation (125), we finally obtain an expression for the stiffness matrix:

$$K = -\rho g B^T \hat{K} B \tag{142}$$

where

$$\hat{K} \int_{z_1}^{z_1+\delta z} (\phi'' \phi''^T + z\phi' \phi'^T)\, dz \tag{143}$$

The matrix $\hat{K}$ can be evaluated by integrating (143) by parts twice and noting (131), which yields

$$\hat{K} = (\phi'' \phi'^T - \phi''' \phi^T + z\phi'\phi^T) \Big|_{z_1}^{z_1+\delta z} \tag{144}$$

The mass matrix M for this finite element is defined by

$$T = \frac{1}{2} \dot{q}^T M \dot{q} \tag{145}$$

T is the kinetic energy of the element.

For the beam element,

$$T = \frac{1}{2} \int_{z_1}^{z_1+\delta z} \rho \dot{y}^2\, dx \tag{146}$$

An analysis analogous to that of the previous section yields

$$M = \int_{\gamma} B^T \hat{M} B \tag{147}$$

and

$$M = \int_{z_1}^{z_1+\delta z} \phi \, \phi^T \, dz \tag{148}$$

and where γ, B and ϕ are defined as before.

The integrals in (148) are evaluated by expanding the integrands in series and integrating term by term. Three terms were taken, since it can be shown that truncation of the series after three terms results in less than .2% error in the elements of $\hat{M}$ for a 20 division finite element model.

The beam shown in figure 22 is divided into N finite elements and is represented by 2N + 2 coordinates x_1. The overall stiffness matrix K is defined by

$$U = \frac{1}{2} x^T K x \tag{149}$$

Equating U to the sum of potential energies of the finite elements, and matching displacements at nodal points, we find that

$$K = \begin{bmatrix}
k_{11}^1 & k_{12}^1 & k_{13}^1 & k_{14}^1 & 0 & 0 & \\
k_{12}^1 & k_{22}^1 & k_{23}^1 & k_{24}^1 & 0 & 0 & \\
k_{13}^1 & k_{23}^1 & k_{33}^1+k_{11}^1 & k_{34}^1+k_{12}^2 & k_{12}^2 & k_{14}^2 & \\
k_{14}^1 & k_{24}^1 & k_{34}^1+k_{12}^2 & k_{44}^1+k_{22}^2 & k_{23}^2 & k_{24}^2 & \cdots \\
0 & 0 & k_{13}^2 & k_{23}^2 & k_{33}^2+K_{11}^3 & k_{34}^2+K_{12}^3 & \\
0 & 0 & k_{41}^2 & k_{42}^2 & k_{34}^2+K_{21}^3 & k_{44}^2+K_{22}^3 & \\
 & & \vdots & & & &
\end{bmatrix} \tag{150}$$

where K_{ij}^{ℓ} denotes the $(i,j)^{th}$ component of the ℓ^{th} finite element stiffness matrix. Similarly, the mass matrix for the beam is given by

$$M = \begin{bmatrix} m_{11}^1 & m_{12}^1 & m_{13}^1 & m_{14}^1 & 0 & 0 & \\ m_{12}^1 & m_{22}^1 & m_{23}^1 & m_{24}^1 & 0 & 0 & \\ m_{13}^1 & m_{23}^1 & m_{33}^1+m_{11}^2 & m_{34}^1+m_{12}^2 & m_{13}^2 & m_{12}^2 & \cdots \\ m_{14}^1 & m_{24}^1 & m_{34}^1+m_{12}^2 & m_{44}^1+m_{22}^2 & m_{23}^2 & m_{24}^2 & \\ 0 & 0 & m_{13}^2 & m_{23}^2 & m_{33}^2+m_{11}^3 & m_{34}^2+m_{12}^3 & \\ 0 & 0 & m_{14}^2 & m_{24}^2 & m_{34}^2+m_{21}^3 & m_{44}^2+m_{22}^3 & \\ & & & \vdots & & & \end{bmatrix} \tag{151}$$

The dynamic equation of motion in matrix form becomes,

$$M\ddot{x} + Kx = Q \tag{152}$$

where

$$Q^T = (F^1, T^1, F^2, T^2, \ldots)$$

gives the forces and torques applied at nodal points.

The boundary condition $y(0) = 0$ is satisfied by specifying the $x_1=0$, thereby reducing the order of (151) by one.

Equation (152) can be written in state-variable format as

$$\begin{bmatrix} \dot{x} \\ \ddot{x} \end{bmatrix} = \left[\begin{array}{c|c} 0 & I \\ \hline -M^{-1}K & 0 \end{array}\right] \begin{bmatrix} x \\ \dot{x} \end{bmatrix} + \begin{bmatrix} 0 \\ \hline M^{-1}Q \end{bmatrix} \tag{153}$$

The normal mode shapes and frequencies of the free vibration problem are the eigenvectors and eigenvalues of the state-variable dynamics matrix.

$$\left[\begin{array}{c|c} 0 & I \\ \hline -M^{-1}K & 0 \end{array}\right] \tag{154}$$

Finding the eigensystem of (154) is not the most economical method of finding the solutions to (152), particularly since the matrices M and K are symmetric and banded; however, the solution to the closed-loop system once feedback control is incorporated is most easily solved in state variable form.

A Fortran program was written to generate the finite element stiffness and mass matrices, assemble these into the overall stiffness and mass matrices, and solve the eigensystem of the state variable matrix (154). The normal mode frequencies for N=10 and 20 divisions of the beam are summarized in table IV. The approximate analytical results and experimental results are included in table IV for comparison. These numbers are based on the following determination of the beam properties.

Table III Beam Characteristics

Material	Stainless Steel
Length	149.875 inches
Width	6 inches
Thickness	1/32 inches
Linear density	0.644 lb/ft
Stiffness	424.352 lb-in^2

Table IV Normal Mode Frequencies (Hz) of Beam

n	Analytical	10 Divisions	20 Divisions	Experimental
0	.301	.308	.308	~.34
1	.728	.755	.755	.75
2	1.27	1.38	1.38	1.37
3	1.98	2.21	2.21	2.15
4	2.92	3.25	3.24	3.16
5	4.08	4.51	4.47	4.38
6	5.49	6.00	5.93	
7	7.13	7.76	7.62	
8	9.03	9.79	9.55	
9	11.16	12.04	11.73	
10	13.54	15.92	14.15	

In the near future, the following improvements to the model will be made:

- The actuator linkage masses will be included. These masses add to the mass matrix at nodal points in a straightforward manner.

- Damping will be modeled. A common problem with high performance control systems is instability of high frequency modes. Since damping is instrumental in the stability of these modes, it should be included in the model during the design process.

6.3 Control System Hardware and Software

In addition to the flexible beam, a variety of other components are required to complete the flexible beam facility. In the order they will be discussed, sensors, actuators, a microcomputer, microcomputer interfaces, and control software development, constitute a part of the completed facility.

Both an optical position sensor and an eddy current position sensor reached the final selection phase. Many other possibilities were eliminated by the requirement of minimum sensor interaction with the beam dynamics. In order to minimize the effects of external disturbances, the developmental period, and the final cost, an eddy current sensor made by Kaman Science Corporation was selected.

The final actuator selection was a brushless DC torque motor manufactured by Aeroflex Laboratories, Inc. With a three inch moment arm, and the appropriate mechanical linkages, the actuator has the capability of applying five ounces of force to the beam for a maximum one amp input, according to the manufacturer's specifications.

The purpose of the microcomputer in the control loop is to sample the sensors, pass this sampled data through a digital filter, and send the filtered data to the actuators. Assuming a general format for the

digital filter

$$x_{k+1} = \phi\ x_k + K\ z_k$$

$$u_k = C\ x_k$$

The amount of computation is roughly $n^2+np+nm$ multiplications. For the state vector larger than either the number of sensors or actuators, the amount of computation is governed by the n^2 term. Currently available eight bit microprocessors are capable of performing one fixed point double precision software multiply in one millisecond, and one hardware floating point multiply in one hundred microseconds. Due to the limitation imposed by the sampling theorem (i.e. sample two or more times per cycle) the maximum number of controlled modes with software arithmetic is four, and the maximum number using hardware arithmetic is eight.

The microcomputer chosen for the control function is the SYM-1 by Synertek System Corporation. It is based on the 6502 microprocessor and has provisions for 4 K of random access memory (RAM) and 6 K of read only memory (ROM). Additionally, a KIMSI Interface/Motherboard by Forethought Products has been added for interfacing directly to S-100 products, specifically the digital to analog converters, and the hardware arithmetic.

The physical interface between the analog sensors and actuators, and the digital microprocessor is accomplished through D/A and A/D hardware and appropriate buffer circuitry. Sensor sampling is performed under computer control. The twelve bit analog-to-digital (A/D) conversion is a successive approximation technique performed in software with the use of a Vector Graphic Precision Analog Interface Board (PAIB). Similarly, the twelve bit digital-to-analog (D/A) conversion is performed in hardware on the PAIB.

Sensor buffer/amplifiers were used between the sensor output and the computer. The circuit has a high input impedance and eliminates high frequency noise and DC offsets. The scale factor from position to voltage at the A/D converter is five volts per inch. The sensor bandwidth is greater than thirty hertz.

The actuator driver presents a high input impedance to the microcomputer D/A converter and eliminates the high frequency D/A conversion noise and DC offsets from the actuator command. Current feedback is used to eliminate the inductive effects of the torquer. The scale factor from the force applied to the beam to the D/A voltage output is one ounce per volt. The actuator bandwidth is greater than thirty hertz.

Software has been developed to implement the general digital filter discussed in the section on microcomputers. The entire program resides in 2516 erasable programmable ROM by Texas Instruments, and is located on the computer. When the software is initiated, the computer samples the sensors, updates the state estimate, and outputs the control. Data for the program is loaded into RAM and consists of Φ, C, and K, and the dimensions of these matrices. The exact sample period, T, (in msec) is given by

$$T = 0.983\ n^2 + 0.963\ np + 0.963\ nm + 0.258\ n + 0.154\ m + 0.597\ p + 0.010\ m^2 + 0.725\ .$$

A listing of the assembly language software can be found in the Appendix.

6.4 Control Law Design

A variety of control laws may be implemented using the general software discussed in the section on microcomputers. The particular approach used in the initial control law design (and the example presented here), is an implementation of a discrete Kalman filter using a sixth order estimator.

The controller is based on the discretized version of the following continuous system

$$\begin{aligned} \dot{x} &= F\,x + G\,u + \Gamma\,\omega \\ u &= C\,x \\ z &= H\,x + v \end{aligned} \tag{156}$$

where

$$x^T = [q_o, \dot{q}_o, q_1, \dot{q}_1, q_2, \dot{q}_2]$$

$$F = \begin{bmatrix} 0 & 1 & 0 & 0 & 0 & 0 \\ 3.55 & 0 & 0 & 0 & 0 & 0 \\ 0 & 0 & 0 & -1 & 0 & 0 \\ 0 & 0 & 21.60 & 0 & 0 & 0 \\ 0 & 0 & 0 & 0 & 0 & -1 \\ 0 & 0 & 0 & 0 & 68.72 & 0 \end{bmatrix}$$

With a single position sensor and a single force actuator at the free end

$$H = [1 \quad 0 \quad 1 \quad 0 \quad 1 \quad 0]$$

$$G^T = \Gamma^T = [0 \quad 0.18 \quad 0 \quad 0.18 \quad 0 \quad 0.18]$$

This control gains, C, and the estimator gains K are determined by minimizing the appropriate performance index J. In the case of the control problem

$$J = \int_0^\infty (x^T A x + u^T B u) \, dt$$

and for this particular example

$$A = \begin{bmatrix} 1 & & & & & \\ & 0 & & 0 & & \\ & & 1 & & & \\ & & & 0 & & \\ & & & & 1 & \\ & 0 & & & & 0 \end{bmatrix}, \quad B = 0.0025$$

For the estimation problem

$$J = \int_0^\infty (w^T Q^{-1} w + v^T R^{-1} v) \, dt$$

and for this particular example

$$Q = E(w\ w^T) = 10^{-4} \qquad (m/sec^2)^2\ sec$$

$$R = E(v\ v^T) = 10^{-6} \qquad (m)^2\ sec$$

For a six state estimator, one control, and one sensor,

$$T = 0.049978 \text{ sec.}$$

Using a discrete optimal system synthesis DOPTSYS[16] algorithm, the following results are obtained

$$\phi = \begin{bmatrix} 0.950 & 0.047 & -0.045 & -0.000 & -0.044 & -0.000 \\ -0.251 & 0.910 & -0.085 & -0.033 & -0.053 & -0.019 \\ -0.019 & -0.002 & 0.953 & 0.048 & -0.018 & -0.000 \\ -0.064 & -0.084 & -1.144 & 0.939 & -0.044 & -0.019 \\ -0.011 & -0.002 & -0.011 & -0.000 & 0.904 & 0.048 \\ -0.059 & -0.082 & -0.068 & -0.032 & -0.374 & 0.896 \end{bmatrix}$$

$$K = \begin{bmatrix} 0.0438 \\ 0.0265 \\ 0.0183 \\ 0.0165 \\ 0.0103 \\ 0.0110 \end{bmatrix}$$

$$C^T = \begin{bmatrix} -5.3744 \\ -9.4553 \\ -6.5416 \\ -3.7488 \\ -3.0469 \\ -2.2154 \end{bmatrix}$$

and the equivalent frequency domain eigenvalues of the closed loop system are given by

$$-0.85 \pm 2.07\ j \qquad -0.38 \pm 4.66\ j \qquad -0.21 \pm 8.29\ j$$

$$\xi_o = 0.38 \qquad \xi_1 = 0.082 \qquad \xi_2 = 0.025$$

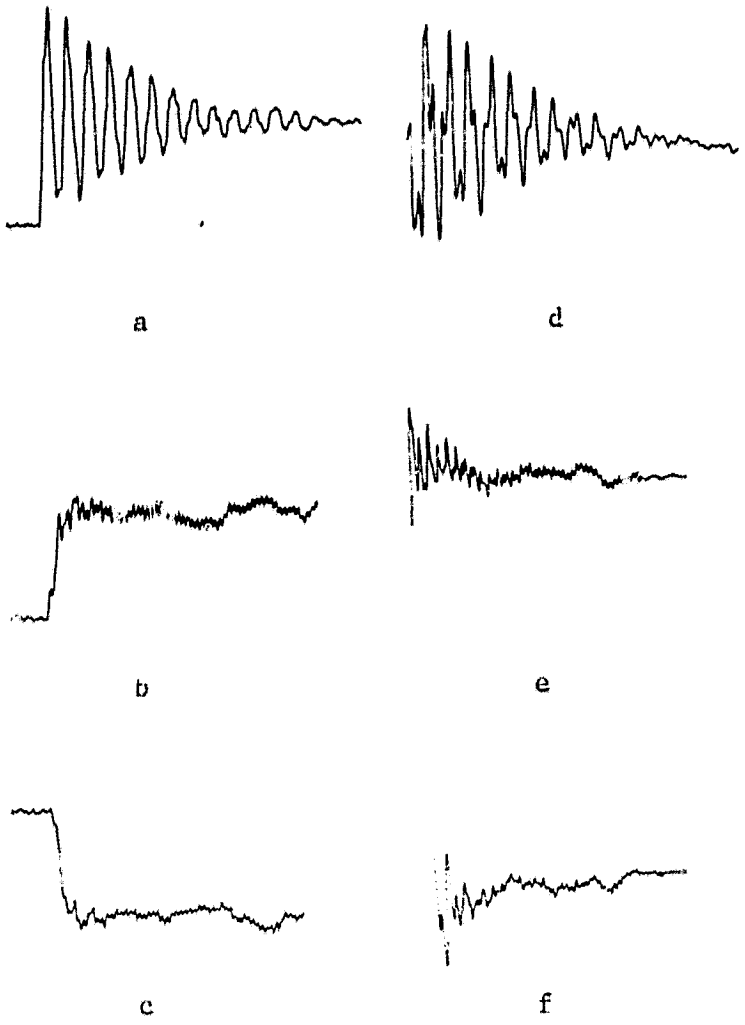

Figure 24. Controlled and Uncontrolled Beam Responses
Amplitude = 1/2 Actual Displacement
Time Scale = 1 sec/cm

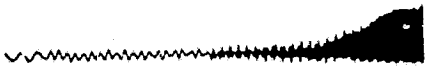

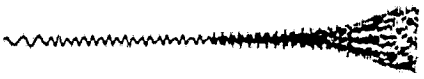

Figure 25. Unstable Control System
Amplitude = 1/2 Actual Displacement
Time Scale = 1 sec/cm

These matrices are converted to the sixteen bit fixed point format used by the microcomputer and are loaded into the controller as data.

The results for this controller can be found in figure 24. Figure 24 contains the uncontrolled and controlled responses to both an initial condition error on positions and to an impulse force input.

Figure 24a shows the open loop response to an initial position error. The majority of the response is the lowest frequency, pendulum mode. It has an open loop damping ratio of -2%.

Figure 24b shows the closed loop response to the same input as in figure 24a, using the controller described previously. Notice the much faster decay rate of the closed loop system. The corresponding control force applied to the beam is shown in figure 24c.

It is now possible to partially verify the control analysis. The predicted closed loop damping ratio for the low frequency mode is 0.38. Using the maximum overshoot of the closed loop position response for determining the closed loop damping ratio, the closed loop damping ratio of 0.40 is experimentally obtained.

Figures 24d, 24e, and 24f show analogous responses of the beam to an impulse force disturbance applied at the free end.

One additional feature present in the closed loop responses in figure 24 is the high frequency oscillation appearing at the tail of each plot. This phenomenon is due to control/observation spillover into the first unmodeled mode at two hertz.

The deleterious effects of spillover in control system design can be demonstrated in the following example. By decreasing the cost of the squared control by a factor of eight, a second control system can be designed and implemented. The results of this control system are shown in figure 25.

In this case the control spillover into the first unmodeled mode is sufficient to drive the system unstable.

Section 7

7.0 Future Work

Future work in the distributed control of large space structures will be concentrated in two areas: (1) extending the distributed control analytical techniques to include general (FE) models and (2) expanding the experimental test facility.

Distributed control analytical techniques will be extended by replacing the continuum models (if needed) used for understanding the theory, with more realistic FE models. Since the theory developed using PDE models will apply to any linear operator, the extension of the finite element models will be straightforward.

The flexible beam test facility will be expanded to an interactive facility. This will allow a general user to work at the computer terminal, design shape and/or active control systems, to implement these control systems with the microprocessor control system, and to obtain graphic outputs and chart recordings of the final results.

References

1. Balas, Mark J., "Active Control of Flexible Systems," AIAA Symposium on Dynamics and Control of Large Flexible Spacecraft, Blacksburg, VA., June 1977.

2. Knox, J.R., and J.M. McCarty, "Algorithms for Computation of Optimal Constrained Output Feedback for Multivariable Flight Control System," AIAA G & C Conference, August 7-9, 1978, Palo Alto, California.

3. Kosut, R., "Suboptimal Control of Linear Time-Invariant Systems Subject to Control Structure Constraints," IEEE Transactions of Automatic Control-15, (1970) p. 557-563.

4. Spalding, G.R., "A State-pace Model for Distributed System," AIAA Astrodynamics Conference, August 7-9, 1978, Palo Alto, California.

5. Ginter, S., and M. Balas, "Attitude Stabilization of Large Flexible Spacecraft," AIAA G & C Conference, August 7-9, 1978, Palo Alto, California.

6. Bryson, A.E., and Y.C. Ho., Applied Optimal Control, Blaisdell, Waltham, Mass., 1969.

7. Levine, N., and M. Athans, "On the Determination of the Optimal Constant Output Feedback Gains for Linear Multivariable Systems," IEEE Transactions of Automatic Control-15, (1970), p. 44-48.

8. Gupta, K.K., "Development of the Program EIGSOL - A Generalized Eigenproblem Solution Routine," Jet Propulsion Laboratory, Pasadena, California, Interoffice Memo 3545;78;310, November 27, 1978 (JPL internal document).

9. Gupta, K.K., "EigenProblem Solution of Damped Structural Systems," International Journal of Numerical Methods in Engineering, Vol. 8, 877-911, 1974.

10. Bryson, A.E., and W.E. Hall, Jr., "Optimal Control and Filter Synthesis by Eigenvector Decomposition," SUDAAR 436, Stanford University, Dec. 1971.

11. Breakwell, John A., "Optimal Control of Flexible Spacecraft Without Model Truncation," Ph.D. Dissertation, Stanford Univ., June 1980.

12. Balakrishnan, A.V., Applied Functional Analysis, Springer-Verlag, New York N.Y., 1976.

13. Rodriguez, Guillermo, "Optimal Control of Large Structures Modeled by Partial Differential Equations," AIAA Guidance and Control Conference, Boulder, Colorado, 1979.

14. Stakgold, I., Boundary Value Problems of Mathematical Physics, Macmillan, New York, 1967.

15. Roach, G.F., Green's Functions: Introductory Theory with Applications, Van Nostrand, London, 1970.

16. Powell, J.E., "Notes on Using Disc for Discrete Control and Filter Synthesis," Stanford University, Spring 1977.